



**HAL**  
open science

## Novel Aquaporin Regulatory Mechanisms Revealed by Interactomics

Jorge Bellati, Chloé Champeyroux, Sonia Hem, Valerie Rofidal, Gabriel Krouk, Christophe Maurel, Veronique Santoni

► **To cite this version:**

Jorge Bellati, Chloé Champeyroux, Sonia Hem, Valerie Rofidal, Gabriel Krouk, et al.. Novel Aquaporin Regulatory Mechanisms Revealed by Interactomics. *Molecular and Cellular Proteomics*, 2016, 15 (11), mcp.M116.060087. 10.1074/mcp.M116.060087 . hal-01382938

**HAL Id: hal-01382938**

**<https://hal.science/hal-01382938>**

Submitted on 15 Mar 2021

**HAL** is a multi-disciplinary open access archive for the deposit and dissemination of scientific research documents, whether they are published or not. The documents may come from teaching and research institutions in France or abroad, or from public or private research centers.

L'archive ouverte pluridisciplinaire **HAL**, est destinée au dépôt et à la diffusion de documents scientifiques de niveau recherche, publiés ou non, émanant des établissements d'enseignement et de recherche français ou étrangers, des laboratoires publics ou privés.



Distributed under a Creative Commons Attribution 4.0 International License

# Novel Aquaporin Regulatory Mechanisms Revealed by Interactomics\*<sup>§</sup>

Jorge Bellati<sup>‡</sup>, Chloé Champeyroux<sup>‡</sup>, Sonia Hem<sup>‡</sup>, Valérie Rofidal<sup>‡</sup>, Gabriel Krouk<sup>‡</sup>, Christophe Maurel<sup>‡</sup>, and Véronique Santoni<sup>‡§</sup>

PIP1;2 and PIP2;1 are aquaporins that are highly expressed in roots and bring a major contribution to root water transport and its regulation by hormonal and abiotic factors. Interactions between cellular proteins or with other macromolecules contribute to forming molecular machines. Proteins that molecularly interact with PIP1;2 and PIP2;1 were searched to get new insights into regulatory mechanisms of root water transport. For that, an immuno-purification strategy coupled to protein identification and quantification by mass spectrometry (IP-MS) of PIPs was combined with data from the literature, to build thorough PIP1;2 and PIP2;1 interactomes, sharing about 400 interacting proteins. Such interactome revealed PIPs to behave as a platform for recruitment of a wide range of transport activities and provided novel insights into regulation of PIP cellular trafficking by osmotic and oxidative treatments. This work also pointed a role of lipid signaling in PIP function and enhanced our knowledge of protein kinases involved in PIP regulation. In particular we show that 2 members of the receptor-like kinase (RLK) family (RKL1 (At1g48480) and Feronia (At3g51550)) differentially modulate PIP activity through distinct molecular mechanisms. The overall work opens novel perspectives in understanding PIP regulatory mechanisms and their role in adjustment of plant water status. *Molecular & Cellular Proteomics* 15: 10.1074/mcp.M116.060087, 3473–3487, 2016.

The absorption of soil water by roots is crucial for plants to maintain their water status. Studies in various plant species have shown that the root water permeability (root hydraulic conductivity;  $L_p$ )<sup>1</sup> is constantly adjusted depending on the

This is an open access article under the [CC BY](https://creativecommons.org/licenses/by/4.0/) license.

From the <sup>‡</sup>Biochimie et Physiologie Moléculaire des Plantes, Institut de Biologie Intégrative des Plantes, UMR 5004 CNRS/UMR 0386 INRA/Montpellier SupAgro/Université Montpellier, F-34060 Montpellier, Cedex 2, France

Received April 1, 2016, and in revised form, August 31, 2016

Published, MCP Papers in Press, September 8, 2016, DOI 10.1074/mcp.M116.060087

Author contributions: V.S. designed research; J.B., C.C., S.H., V.R., and G.K. performed research; J.B., C.C., S.H., V.R., G.K., C.M., and V.S. analyzed data; C.M. and V.S. wrote the paper.

<sup>1</sup> The abbreviations used are:  $L_p$ , root hydraulic conductivity; ABA, abscisic acid; BR, brassinosteroid; FLIM, Fluorescence Lifetime Imaging Microscopy; FRET, Förster resonance energy transfer; GO, Gene Ontology; IP, immuno-purification; LRR, Leucine-rich-repeat;

developmental stage of the plant, its nutritional or hormonal status, or multiple environmental stimuli (1, 2). These adjustments depend in large part on the function and regulation of aquaporins, a large class of channel proteins that facilitate the diffusion of water and small neutral solutes across cell membranes (2, 3). Aquaporins are 25–30 kDa proteins with 6 membrane-spanning domains and five connecting loops (A–E), the N- and C-terminal tails being exposed to the cytosol (4). Plant aquaporins show a high multiplicity of isoforms. Thirty-five homologs comprised in four homology subclasses have been identified in *Arabidopsis*. The plasma membrane intrinsic proteins (PIPs) (with 13 isoforms further subdivided in the PIP1 and PIP2 subgroups), and the tonoplast intrinsic proteins (TIPs) (with 10 homologs) are the most abundant aquaporins in the plasma membrane and the tonoplast, respectively (5, 6). Two other subclasses include nodulin-26-like proteins (NIPs) and small basic intrinsic proteins (SIPs), with nine and three homologs, respectively (5–7).

The response of plant roots to environmental and hormonal stimuli is mediated through long-term transcriptional control of aquaporin functions, together with multiple post-translational mechanisms, such as phosphorylation, that affect the activity of aquaporins, their targeting to their destination compartment, or their stability. PIP aquaporins show a conserved phosphorylation site in their first cytosolic loop (loop B) and, in the case of PIP2 isoforms, multiple phosphorylations in adjacent sites of their C-terminal tail (1), PhosPhAt database (<http://phosphat.mpimp-golm.mpg.de/>). Aquaporin phosphorylation is a significant component of plant responses to stresses. For instance, following exposure of *Arabidopsis* roots to salt (NaCl) or hydrogen peroxide (H<sub>2</sub>O<sub>2</sub>), AtPIP2;1 phosphorylation was decreased and increased, respectively (8). A recent quantitative phosphoproteomic work showed a strong correlation between the level of PIP phosphorylation and  $L_p$ , under a wide range of environmental conditions (1). However, knowledge of the protein kinases (PKs) that phosphorylate aquaporins is still scarce. Two PKs that phosphorylate SoPIP2;1 at Ser<sup>115</sup> and Ser<sup>274</sup> have been purified from

NIP, nodulin-26-like protein; PA, phosphatidic acid;  $P_i$ , osmotic water permeability; PIP, plasma membrane intrinsic protein; PK, protein kinase; RLK, receptor-like-kinase; SIP, small basic intrinsic protein; TIP, tonoplast intrinsic protein; TSPO, tryptophan-rich sensory protein/translocator.

spinach (9). A very recent work revealed that Open stomata 1 (OST1)/Snf1-related PK 2.6 (SnRK2.6), a central PK in guard cell abscisic acid (ABA) signaling, was able to phosphorylate a cytosolic AtPIP2;1 peptide at Ser<sup>121</sup>, this modification being necessary during ABA-induced stomatal closure (10). Receptor-like-kinases (RLKs) constitute a class of serine/threonine kinases that perceive environmental and extracellular developmental signals and transduce them *via* their intracellular kinase domain (11). Two RLKs, SIRK1 (At5g10020) and BSK8 (At5g41260), a leucine-rich-repeat (LRR)-RLK and a receptor-like cytoplasmic kinase (RLCK), respectively, were shown to act on PIPs (12, 13). In particular, phosphorylation of five PIPs (AtPIP2;1–2;4, AtPIP2;7) upon stimulation by sucrose of carbon-starved seedlings was reduced in the *sirk1* mutant, and *SIRK1* was confirmed to phosphorylate AtPIP2;4 at Ser<sup>283</sup> and Ser<sup>286</sup>. A rice RLK (LP2, Os02g40240), was recently shown to interact with three PIPs *in vivo* (14) but the functional role of this interactions remains unknown.

The identification of cellular interaction partners is fundamental for understanding cellular and physiological processes. In recent years, crucial experimental approaches for protein interaction mapping such as yeast two hybrid or split ubiquitin, have begun to unravel the complex interacting networks of plant proteins (15–18). Analysis of protein complexes through immuno-purification (IP) followed by mass spectrometry (MS) (19) is also a widely employed technique because of its high throughput and sensitivity. Most importantly, this technique addresses the properties of protein-protein interactions occurring in the plant. However, suitable controls and quantitative proteomics are required to distinguish between bona fide binders and background contaminants (20).

Data on plant aquaporin interactomes are starting to emerge. Yeast-two hybrid (18) and split-ubiquitin (15, 16) studies have identified, about 200 proteins that seem to interact, with a high confidence, with PIP aquaporins ((21) for review). In addition, more focused recent studies have revealed that PIPs can functionally interact with several classes of proteins. For instance, PIP1-PIP2 interactions were shown to be required for *in planta* trafficking of PIP1s to the plasma membrane (22–24). PIP2s were also shown to functionally interact with syntaxins, a family of proteins involved in vesicle trafficking (25, 26). In addition, the tryptophan-rich sensory protein/translocator (TSPO), a multistress regulator that is transiently induced by osmotic stress, and that is degraded through a selective autophagic pathway, physically interact with AtPIP2;7 (27). PIPs also functionally interact with Rma1H1, a membrane-anchor E3 ubiquitin ligase homolog, to regulate aquaporin levels *via* ubiquitination (28).

One major objective of the present work was to investigate as a whole the plant PIP1;2 and PIP2;1 interactome. A quantitative IP-MS strategy, together with data from available databases, allowed to build an interconnected PIP network of about 900 proteins. Next, we focused on those protein interaction partners (next called interactants) that show a physical

interaction with PIPs. We hypothesized that these interactants may provide novel insights into the molecular regulation of PIP aquaporins. Here, we explore novel functional roles of phospholipases D and RLKs. The latter can have opposite effects on aquaporin activity through specific molecular mechanisms.

#### EXPERIMENTAL PROCEDURES

**Biological Materials and Plant Treatments**—*Arabidopsis thaliana* (Col-0 ecotype) transgenic plants expressing GFP, GFP-PIP2;1, GFP-PIP1;2 under the control of a constitutive <sup>35</sup>S promoter were used (29) for proteomic analysis (see below). *Arabidopsis* seeds were sown *in vitro* on a MS/2 medium (30) complemented with 1% sucrose, 0.05% MES and 7 g/l agar. Seeds were kept at 4 °C for 48 h and cultivated *in vitro* during 9 days (16 h light (250 μmol photons/m<sup>2</sup>/s), 20 °C, 70% relative humidity). The effect of NaCl and H<sub>2</sub>O<sub>2</sub> were studied by bathing plantlets with 100 mM NaCl during 2 h, and 500 μM H<sub>2</sub>O<sub>2</sub> for 20 min, respectively. Additional transgenic plants were used: promAMT1;3::AMT1;3-GFP (31), promPGP4::PGP4-GFP in a *gpg4* background (32), promPGP19::GFP-PGP19 (33). *Nicotiana tabacum* plants were cultivated in soil for 4–6 weeks (8 h light (120 μmol photons/m<sup>2</sup>/s), 20 °C, 65% relative humidity).

**Vectors and Constructs**—All constructs were obtained using Gateway cloning technology (Invitrogen) according to the manufacturer's instructions. The cDNAs of RKL1 (At1g48480), RLK902 (At3g17840), Feronia (At3g51550), PLDδ (At4g35790), PLDγ1 (At4g11850), and NHL3 (At5g06320) were amplified by PCR using the primers described in supplemental Table S1 followed by a second PCR with the primers AttB1 or AttB1' and AttB2 or AttB2' (supplemental Table S1) allowing the addition of attB recombination sites and cloned into a pDONOR 207 vector using a Gateway® BP Clonase enzyme mix (Invitrogen). Annexin4 clone (At2g38750) was obtained from ARBC (U15576 clone). For FLIM experiments, cDNAs were transferred into binary destination vectors pGWB5 and pGWB6 (Dr. Nakagawa, Shimane University, Matsue, Japan) to allow fusion of eGFP at the C- and N terminus of the proteins of interest, respectively, by using a Gateway® LR Clonase enzyme mix (Invitrogen). To fuse mRFP at the C terminus of the proteins, cDNAs were transferred into a pB7WGR2 vector. GFP- and mCherry- tagged PIP2;1 are described in (34, 35). *A. tumefaciens* strain GV3101 was transformed with the constructs of interest, selected for resistance toward rifampicin (50 mg/l), gentamycin (25 mg/l), and kanamycin (50 mg/l) in the case of pGWB vectors, and for resistance toward spectinomycin (100 mg/l) in the case of pB7WGR2 vector. For oocytes experiments, cDNAs were transferred into a *xenopus* oocyte expression vector pGEM-GWC using a Gateway® LR Clonase enzyme mix (Invitrogen) and *E. Coli* strain DH5α was transformed and selected for ampicillin (50 mg/l) resistance.

**Immunopurification**—IP of GFP-tagged proteins was performed at 4 °C from 9 day-old plantlets. Plantlets were treated with 1% formaldehyde for 15 min under gentle shaking. Formaldehyde was then quenched with the addition of 300 mM glycine under continuous shaking. After for 30 min, plantlets were rinsed twice with phosphate-buffered saline (4 mM KH<sub>2</sub>PO<sub>4</sub>, 16 mM Na<sub>2</sub>HPO<sub>4</sub>, 115 mM NaCl, pH 7.4). One to two grams of roots were collected, chopped with a scalpel in the presence of 2.1 ml/g fresh weight (FW) of a buffer made of NaCl 300 mM, Triton X-100 1% (w/v), Na deoxycholate 0.5% (w/v), SDS 0.1% (w/v), Tris-HCl 100 mM pH 8, leupeptin 2 mM, DTT 5 mM, AEBSF 1 mM, and then potterised. After centrifugation at 10,000 × g for 15 min, the supernatant was again centrifuged in the same conditions. IP was performed from the supernatant with an antibody against GFP using a μMACS™ anti-GFP Microbeads kit (Miltenyi Biotec, Paris, France) according to manufacturer's conditions. Briefly,

sample was incubated at 4 °C for 1 h with a volume equivalent to 35  $\mu$ l/g FW of an anti-GFP Microbeads solution. The sample was then loaded onto  $\mu$ MACS columns that were previously conditioned with 200  $\mu$ l of a lysis buffer (NaCl 150 mM, Triton X-100 1% (w/v), Tris-HCl 50 mM pH 8). After 4 washings with 200  $\mu$ l of a buffer made of NaCl 150 mM and Igepal CA-630 1% (v/v) and an additional washing step with 100  $\mu$ l of Tris-HCl 20 mM pH 7.5, proteins were eluted with 50  $\mu$ l of elution buffer (Tris-HCl 50 mM pH 6.8, DTT 50 mM, SDS 1% (w/v), EDTA 1 mM, bromophenol blue 0.005% (v/v), glycerol 10% (v/v)). Formaldehyde fixation was reversed by heating eluted proteins at 100 °C during 20 min.

**Protein Digestion**—In-solution reductions/alkylations were performed simultaneously with detergent removing by the filter-aided sample preparation protocol (1, 36). These steps were followed by an endolysin-C (Sequencing Grade Modified, Promega, Madison, WI) digestion 3 h at 37 °C followed by a trypsin (Sequencing Grade Modified, Promega) digestion overnight at 37 °C. Peptides were eluted by step elutions with 50 mM ammonium bicarbonate, followed by 50% acetonitrile and then 0.5 M NaCl. Peptides were desalted on C18 columns (Sep-Pak® VactC18 cartridge 3cc, Waters, Guyancourt, France). After solvent evaporation, peptides were resuspended in 2% formic acid.

**Experimental Design and Statistical Rational for Protein Identification and Quantification by Mass Spectrometry**—The protein digests were analyzed using a Q-TOF mass spectrometer (Maxis Impact; Bruker Daltonik GmbH, Bremen, Germany), interfaced with a nano-HPLC U3000 system (Thermo Scientific, Waltham, MA). Samples were concentrated with a pre-column (Thermo Scientific, C18 Pep-Map100, 300  $\mu$ m  $\times$  5 mm, 5  $\mu$ m, 100 Å) at a flow rate of 20  $\mu$ l/min using 0.1% formic acid. After preconcentration, peptides were separated with a reversed-phase capillary column (Thermo Scientific, C18 PepMap100, 75  $\mu$ m  $\times$  250 mm, 3  $\mu$ m, 100 Å) at a flow rate of 0.3  $\mu$ l/min using a two steps gradient (8% to 28% acetonitrile in 40 min, then 28% to 42% in 10 min), and eluted directly into the mass spectrometer. Proteins were identified by MS/MS by information-dependent acquisition of fragmentation spectra of multiple charged peptides. Up to twenty data-dependent MS/MS spectra were acquired in positive ion mode. MS/MS raw data were analyzed using Bruker Compass Data Analysis software (Automatic Engine Version 4.1 (Build 359)) to generate the peak lists. The non-redundant *Arabidopsis* protein database (TAIR10, version 20110823, 35386 entries, <http://www.arabidopsis.org>) was locally queried using X!Tandem search engine (version 2013.09.01; <http://www.thegpm.org/tandem/>) with the following parameters: trypsin as enzyme, 1 allowed missed cleavage, carbamidomethylation of cysteine as fixed modification and N-terminal acetylation of protein, deamidation of asparagine and glutamine, N-terminal-pyroglutamylation of glutamine and glutamate, oxidation of methionine, phosphorylation of serine, threonine and tyrosine, and methylation of glutamate and aspartate as variable modifications. Mass tolerance was set to 10 ppm on full scans and 0.05 Da for fragment ions. Identified proteins were filtered and grouped using the X!Tandem pipeline v3.3.1 (<http://pappso.inra.fr/bioinfo/xtandempipeline/>). Identified proteins were filtered according to the following criteria: at least two different trypsin peptides with an *E* value below 0.05 and a protein *E* value smaller than 0.025 were required. Using the above criteria, the rate of false peptide sequence assignment and false protein identification as determined by the “decoy database” function implemented in X!Tandem pipeline was lower than 1.5 and 5%, respectively. The X!Tandem grouping function allows to take into account redundancy and proteins with at least one common peptide were grouped. Within each group, proteins with at least one specific peptide relative to other members of the group were reported as subgroups. Relative label-free quantification was carried out with the MassChroQ software (version 2.1) based on extracted ion

chromatograms (37). The detection threshold was set at a minimal and maximal value of 3000 and 5000, respectively. Data were filtered to remove (1) unreliable peptides for which standard deviation of retention time was above 15 s, (2) peptides shared within several proteins, and (3) quantified peptides in less than 3 biological replicates. Normalization was performed to take into account putative global quantitative variations between LC-MS runs. Normalized peptide areas were calculated by dividing the area value of each peptide by the sum of all peptide area values within each LC-MS run. The quantification of a protein relied on the quantification of the sum of its peptides. A Student *t* test (*p* value < 0.05) allowed to determine the significant change in abundance. Then, we also considered proteins identified with a unique peptide provided that this peptide showed a significant quantitative variation within treatments. The mass spectrometry proteomics data have been deposited in ProteomeXchange (<http://proteomecentral.proteomex.org>) (accession number: PXD001000) (38); <http://moulon.inra.fr/protic/pipinteractome> (login: pipinteractome; password: review).

**Data Analysis and Protein Interaction Networks**—The subcellular localization of interactants was predicted with SUBAcon server (<http://suba.plantenergy.uwa.edu.au/>) and the number of transmembrane domains was estimated with Aramemnon (<http://aramemnon.botanik.uni-koeln.de/>). The functional classification of interactants according to Gene Ontology (GO) annotation, and enrichment in interactants with regards to the *Arabidopsis* genome were performed with Panther server (<http://pantherdb.org/>) (39). Protein-protein interaction data were obtained from plant interactome databases including results from a yeast two hybrid approach (18) (*Arabidopsis* Interactome Mapping Consortium, 2011) and from Split-ubiquitin approaches (15, 16) to build a network including PIP interactants identified in the present work together with the reported interactants of these PIP interactants. Protein-protein interaction networks were visualized using Cytoscape (40). Networks were analyzed using the Cytoscape 2.8.2 Molecular Complex Detection (MCODE) plugin (41) to detect clusters (*i.e.* densely connected regions) that are predictive of functional protein complexes. The parameters used for MCODE to generate the clusters were as follows: loops included, degree cut-off of 2, deletion of single connected nodes from the cluster (haircut option disabled), expansion of the cluster by one neighbor shell (fluff option enabled), node density cut-off of 0.1, node score cut-off of 0.2, k-core of 2, and maximum depth of the network equal to 100.

**Fluorescence Lifetime Imaging Microscopy (FLIM)**—For transient expression in leaves, 4- to 6-week-old tobacco (*N. tabacum* cv SR1) plants were infiltrated with *Agrobacterium tumefaciens* strain GV3101 with the desired construct as described previously (42) and exhibiting an optical density at 600 nm between 0.025 and 0.05. Infiltration was performed at an induced wound in leaves to facilitate the transformation. In the case of multiple transformations, transformed agrobacteria were mixed. Tobacco plants were kept in the same culture condition during transient expression. Tobacco epidermal cells were observed on a portion of ~25 mm<sup>2</sup> of transformed leaf 72 h after infiltration. FRET (Förster resonance energy transfer) and FLIM measurements were obtained with a multiphoton confocal microscope (ZEISS LSM 780, Göttingen, Germany) by the so-called TCSPC (Time Correlated Single Photon Counting) method (43). GFP was excited at 920 nm with a pulsed infra-red laser Ti:Saphir (Chameleon ULTRA II, COHERENT) for 3 min. The emitted fluorescence was detected by a detector HPM-100 Hybrid (Hamamatsu R10467–40 GaAsP) in descanned position. The laser synchronization and measurement of photon life time were performed using a capture card SPC-830 (B&H). Cells were selected provided that (1) the fluorescence intensity of mCherry/mRFP was higher than that of eGFP to optimize FRET conditions and (2) cells were isolated from any cell expressing GFP alone, in order not to dilute the FRET signal. One to three biological replicates were

performed by tested couples. For each repetition, 5 to 10 images were obtained and analyzed. From the fluorescence intensity images, the decay curves were calculated per pixel and fitted with either a mono- or double-exponential decay model using the SPCImage software (<http://www.becker-hickl.de/software/tcspc/softwaretcspcspecial.htm>). The mono-exponential model function was applied for donor samples with only GFP present. For samples containing two fluorophores, GFP/mCherry or GFP/RFP, a double-exponential model function was used without fixing any parameter. The lifetime of GFP expressed alone and the lifetime of GFP co-expressed with mCherry or mRFP were compared using Student's *t* test, by grouping all the repetitions for the same couple. The FRET efficiency is calculated according to the following formula:  $FRET = 1 - (GFP \text{ lifetime in the presence of mCherry/RFP}) / (GFP \text{ lifetime expressed alone})$ .

**Oocyte Expression**—cRNA production, expression in *Xenopus laevis* oocytes, and osmotic water permeability ( $P_f$ ) measurements were performed as previously described (44).

## RESULTS

**Interactomics Methodology**—We used an IP method coupled to protein identification by MS to characterize proteins copurifying with PIP1;2 and PIP2;1 (further referred to as PIP1;2 and PIP2;1 interactants). Root extracts were prepared from transgenic plants expressing GFP-PIP2;1 or GFP-PIP1;2 under the control of a  $^{35}\text{S}$  promoter and paramagnetic anti-GFP microbeads were used to purify the fusion proteins and their interacting proteins. This approach was performed in plants grown in standard conditions or treated with salt (100 mM NaCl, 2h) or hydrogen peroxide (500  $\mu\text{M}$   $\text{H}_2\text{O}_2$ , 20 min), two treatments described to inhibit aquaporin activity and root water transport (34, 45). Aquaporins are hydrophobic membrane proteins that require detergents for solubilization. However, these detergents may not be compatible with a proper recovery of interacting proteins. To circumvent this problem, plant tissues were treated with formaldehyde (46) to cross-link protein complexes *in vivo*. A protein was considered as a genuine PIP interactant when it was identified in at least 3 over 4 replicates with at least two significant different peptides (see methods). In addition, an IP-MS/MS from plants expressing  $^{35}\text{S}$ ::GFP allowed to identify 22 GFP interactants that were removed from the initial lists of PIP2;1 and PIP1;2 interactants (supplemental Table S2). Overall, a total of 436 and 388 proteins were identified as putative interactants of PIP1;2 and PIP2;1, respectively (supplemental Tables S3, S4), taken into account all plant physiological treatments.

The identification of similar proteins with independent PPI methodologies can be used to validate true interactants. Previous yeast two-hybrid ([http://interactome.dfci.harvard.edu/A\\_thaliana](http://interactome.dfci.harvard.edu/A_thaliana); *Arabidopsis* interactome mapping consortium 2011, (18)) and split-ubiquitin approaches ([www.associomics.org](http://www.associomics.org), (15, 16)) identified as a whole, 29 and 35 proteins interacting with PIP1;2 and PIP2;1, respectively (supplemental Table S5). Three and five of these PIP1;2 and PIP2;1 interactants, respectively, were also identified in the present work. Among them, five are PIPs (24) whereas others correspond to

a  $\text{Ca}^{2+}$ -ATPase, and sugar or phosphate transporters. This comparative analysis confirms the usually low overlap between binary approaches and whole protein complex analysis (47). A reverse IP-MS strategy was used to confirm the interaction between PIP2;1 and PIP1;2 and a few selected interactants using transgenic plants expressing promAMT1;3::AMT1;3-GFP (31, 48), promPGP4::PGP4-GFP in a *pgp4* background (32), and promPGP19::PGP19-GFP (49). A total of 282, 22, and 31 proteins were identified in the interactomes of AMT1;3, PGP4, and PGP19, respectively (supplemental Tables S6, S7). The bait itself and both PIP1;2 and PIP2;1 were recovered in each interactome, thereby supporting the relevance of IP-MS to identify PIP interactants.

**PIP Interaction Network**—PIP1;2 and PIP2;1 shared about 80% of their interactants (Fig. 1A). Given such a high similarity between the two interactomes, all interactants were further considered as defining a “PIP interactome.” One third of them exhibited at least one transmembrane domain (<http://aramemnon.botanik.uni-koeln.de/>) (supplemental Table S3) and the remaining are soluble proteins possibly bound to membranes. Indeed, 32 and 8% of PIP interactants are predicted to localize to the plasma membrane and endoplasmic reticulum, respectively (<http://suba.plantenergy.uwa.edu.au/>) (supplemental Table S3). Thus, the PIP2;1 and PIP1;2 interactomes are somewhat enriched in proteins sitting in the same subcellular compartments as their bait. According to Gene Ontology annotation (<http://pantherdb.org/>), almost 90% of assigned accessions had catalytic activities, binding activities and belonged to proteins contributing to structural integrity of cellular complexes and to transport activity (Fig. 1B). These functions are clearly over-represented when compared with the *Arabidopsis* genome (Fig. 1B). As for biological processes, metabolic process and localization (Fig. 1C) were predominant, the latter being mostly enriched through the term “vesicle-mediated transport” (Fig. 1C).

Several previous studies pointed to an enrichment of plasma membrane proteins in microdomains according to abiotic, biotic, and chemical treatments (50–53). Interestingly, 22% of PIP interactants ( $n = 106$ ) were shown to be enriched in microdomains in these studies (supplemental Table S3). In addition, PIP interactome contained 38 PKs (supplemental Table S3) including 23 RLKs and 6 calcium-dependent PKs.

Assuming that interacting proteins contribute to similar molecular functions or cellular processes, we next built a network including all PIP interactants identified in the present work or in previous Y2H (18) and Split-Ub approaches (15–17). Hubs are proteins showing multiple protein interactions that may be generated by lowly specific individual interactions (16). Thus, interactants of hub proteins with more than 70 interactants were removed, to prevent corruption of the PIP network with low-affinity interactions. The final network consists of 883 proteins linked by 1620 edges (supplemental Table S8, supplemental Fig. S1). In addition, five main clusters were iden-

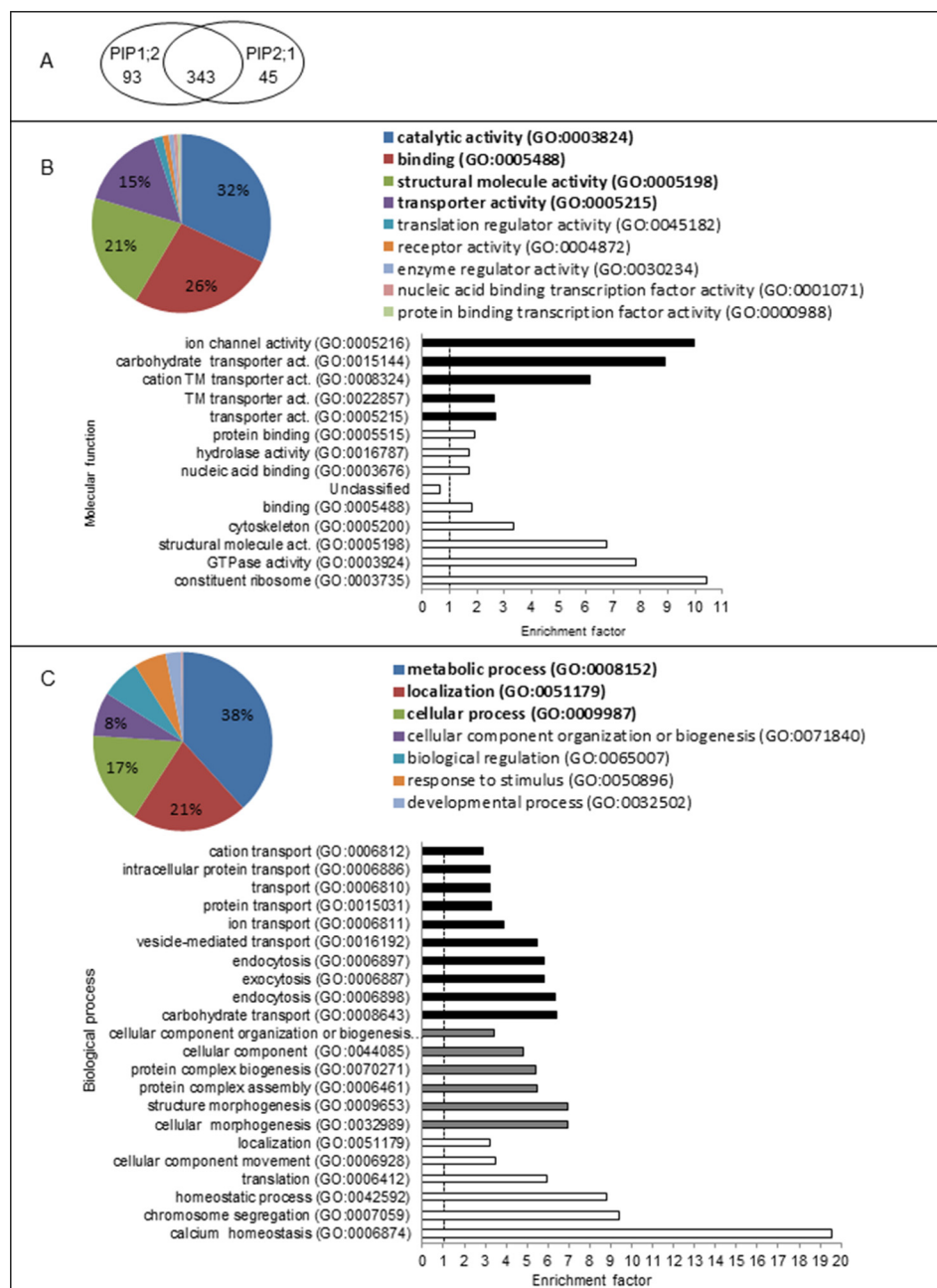


**FIG. 1. PIP1;2 and PIP2;1 interactomes.** A, number of PIP1;2 and PIP2;1 interactants. B, molecular functions characterizing PIP interactants and overrepresented in PIP interactome by comparison to the *Arabidopsis* genome (<http://pantherdb.org/>, (39)). Enriched molecular functions with  $p$  value < 0.05 are shown. Revigo (<http://revigo.irb.hr/>) was used to summarize molecular functions and enriched ones related to transport activity are shown in black. C, biological processes characterizing PIP interactants and over-represented in PIP interactome by comparison to the *Arabidopsis* genome (<http://pantherdb.org/>, (39)). Enriched biological processes with  $p$  value < 0.05 and an enrichment factor > 3 are shown. Enriched biological processes analyzed using Revigo and related to vesicle-mediated transport and cellular component biogenesis are shown in black and gray, respectively.

tified (Fig. 2; supplemental Table S8). Clusters 1, 2, and 3 comprise aquaporins, transporters, and GTPases, respectively, that were already pinpointed in Fig. 1 as enriched molecular functions. Clusters 4 and 5 grouped proteins from exocyst complex or involved in brassinosteroid (BR) signaling, respectively (Fig. 2; supplemental Table S8). The exocyst

complex comprises 8 subunits engaged in docking and tethering of secretory vesicles, providing a spatial and temporal regulation of exocytosis (54, 55). BRs are phytohormones that regulate plant growth and development. Thus, this clustering analysis points to novel functional features of the PIP interactome.

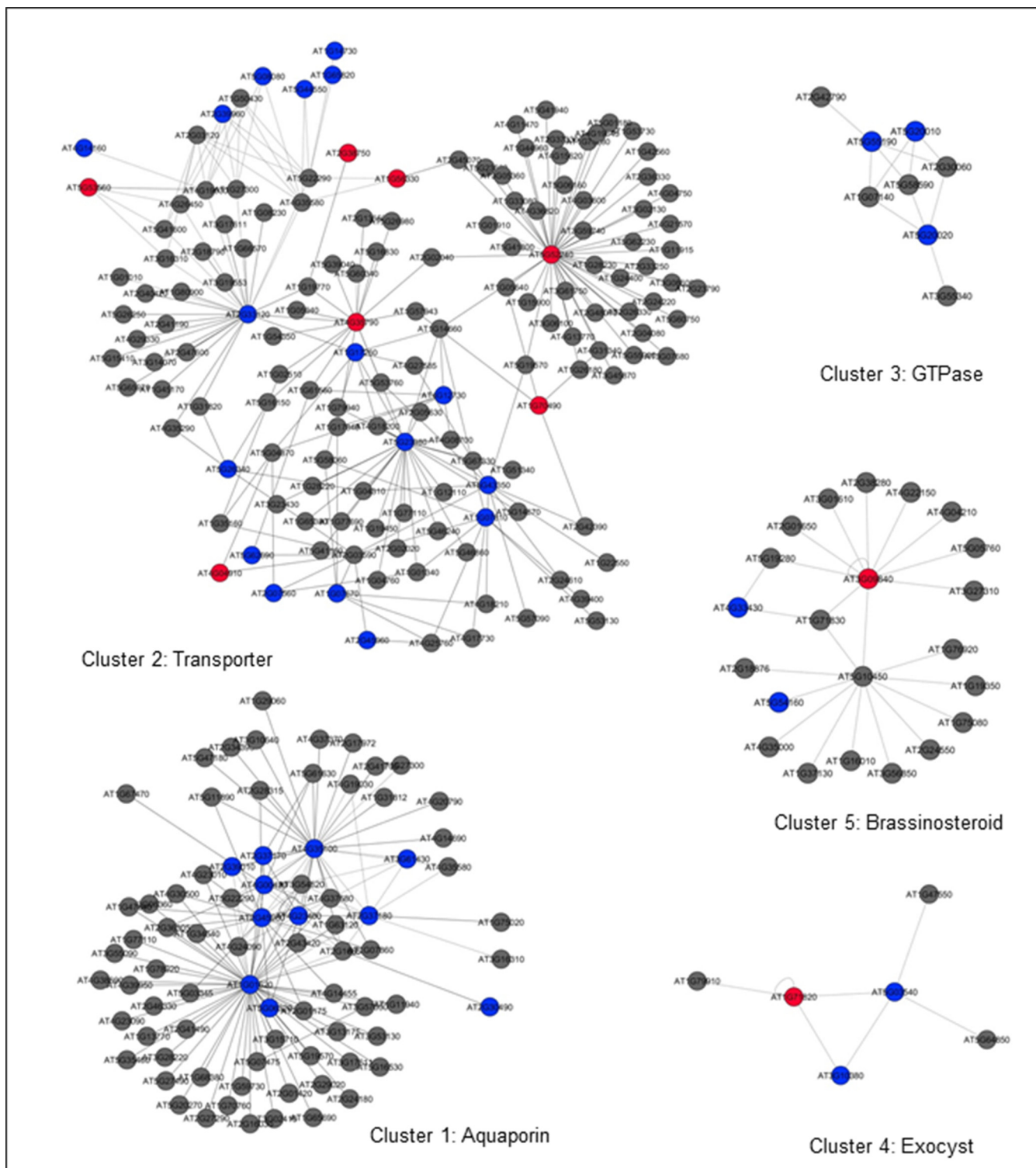
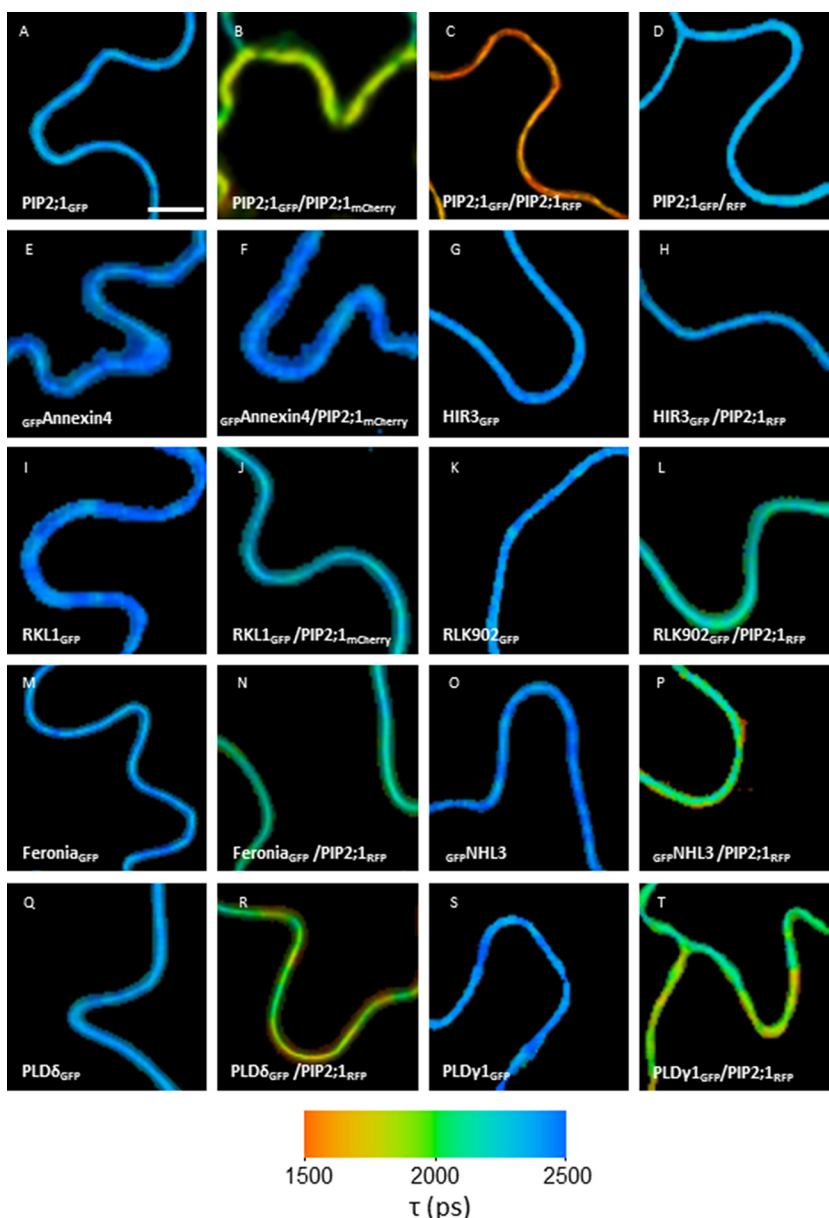


FIG. 2. **Clustering analysis of PIP network.** The MCODE plugin of Cytoscape (41) was used to distinguish 5 major clusters in the PIP network. Corresponding AGI numbers can be found in [supplemental Table S8](#). AGI of proteins are represented by nodes in a color-code way: *Blue*: interactants identified in the present work with no quantitative variations upon treatments. *Red*: interactants identified in the present work with quantitative variations upon treatments. *Gray*: interactants of PIP interactants that are reported in databases. *Solid line*: data from (18); *dashed line*: data from (15, 16).



**FIG. 3. Physical interaction between PIP2;1 and selected members of the PIP interactome.** FLIM technology was used to study the physical interaction between PIP2;1 and Annexin4, HIR3, RKL1, RLK902, Feronia, NHL3, PLD $\delta$ , and PLD $\gamma$ 1. Analyses were performed in leaf epidermal cells transiently expressing fluorescent tagged proteins (A, E, G, I, K, M, O, Q, S) alone or in combination with mCherry- or RFP-tagged proteins (B, D, F, H, J, L, N, P, R, T). Controls for a positive interaction were obtained from the interaction between PIP2;1-GFP and PIP2;1-mCherry (B) and PIP2;1-GFP and PIP2;1-RFP (C). Control for a negative interaction was obtained from the co-expression of PIP2;1-GFP with RFP (D). The donor fluorescence lifetime  $\tau$  was calculated as described under Experimental Procedures and is indicated by a color code from red for  $\tau$  values of 1500 ps to blue for  $\tau$  values of 2500 ps. Values are indicated in Table I. Scale bar: 10  $\mu$ m.

A label-free quantitative mass spectrometry approach was used to measure the variations in abundance of PIP1;2 and PIP2;1 interactants, according to NaCl and H<sub>2</sub>O<sub>2</sub> treatments. Forty-nine and 12 proteins of the PIP1;2 and PIP2;1 interactomes, respectively, responded to NaCl (supplemental Table S3, supplemental Table S4D, S4F) whereas 39 and 38, respectively, showed an altered abundance, in response to H<sub>2</sub>O<sub>2</sub> (supplemental Table S3, supplemental Table S4C, S4E). PIP networks were built considering all PIP interactants with variations in abundance according to H<sub>2</sub>O<sub>2</sub> (H-network) and NaCl (N-network) treatments, and revealed 243 proteins and 182 connected proteins, respectively (supplemental Table S8, supplemental Fig. S2A, S2B). Interestingly, according to GO annotation, those PIP interactants were enriched in vesicle-mediated transport process (GO:0016192) (supplemental Ta-

ble S9) suggesting that the two treatments rather interfere with PIP cellular trafficking.

**Physical Interaction Between Interactants and PIP2;1**—With the objective of identifying proteins that physically act on PIP2;1 function, we selected a subset of plasma membrane localized-proteins, based on their biological function, quantitative variations according to H<sub>2</sub>O<sub>2</sub> and NaCl treatments, putative enrichment in microdomains, or presence in a specific cluster. Putative physical interactions with PIP2;1 were then investigated using FLIM. The prevalence of RLKs (56) in PIP interactome made us consider three of them. RKL1 (At1g48480) and RKL902 (At3g17840) are close homologs belonging to the LRR-RLK family. Expression of RKL902 in root tips and lateral primordia suggests a role in cell proliferation (57). Feronia (At3g51550) is a well-described RLK that

fine-tunes cell growth by controlling apoplastic pH (58) and ROS (59, 60), thereby balancing wall rigidity for cell integrity and flexibility for cell expansion. These are the reasons why RKL1, RLK902, and Feronia were selected despite their abundance was not altered by H<sub>2</sub>O<sub>2</sub> and NaCl treatments. Phospholipases D (PLDs) fulfil diverse roles in lipid metabolism and cellular regulation (61, 62). Here, we selected PLD $\delta$  (At4g35790) and PLD $\gamma$ 1 (At4g11850) that show quantitative variations according to treatments (supplemental Table S3) and are present in cluster 2 of PIP interactome (Fig. 2). Annexin4 (At2g38750) that belongs to the same cluster as PLDs was also selected. In animals, annexins associate with membrane phospholipids and facilitate fusion of cytoplasmic vesicles with the plasma membrane (63) and one of these (annexin A2) mediates c-AMP-induced trafficking of Aquaporin-2 in the collecting duct (64). Finally, we also selected HIR3 because of its localization in microdomains (51, 53) and NHL3 because of its high degree of protein connection (19 proteins including 3 PIPs) (supplemental Fig. S3).

FLIM analyses were performed in tobacco leaf epidermal cells that transiently expressed the two putative interacting partners tagged with GFP and mCherry- or RFP, respectively (Table I, Fig. 3). Physical interactions were assessed based on a significant  $p$  value ( $<0.01$ ), whatever the FRET efficiency. Well established homo-tetrameric interactions of PIPs homologs (24) were used as positive controls. Thus, PIP2;1 fused to GFP showed strong interaction with PIP2;1 fused to RFP and mCherry (Table I, Fig. 3). Negative controls were obtained from coexpression of PIP2;1 fused to GFP with soluble RFP and with HIR3 (At3g01290) that is an anchored membrane protein (Table I, Fig. 3). Whereas no relevant physical interaction could be detected between PIP2;1 and Annexin4, a significant physical interaction was revealed between PIP2;1 and 3 RLKs (RKL1, RLK902, and Feronia), two PLDs (PLD $\delta$  and PLD $\gamma$ 1), and NHL3 (At5g06320) (Table I, Fig. 3).

**RKL1, RLK902, and Feronia Modulate PIP2;1 Intrinsic Water Transport Activity**—With regard to their putative PK function, RKL1, RLK902, and Feronia were chosen for further investigating a functional role on PIP2;1 activity, using coexpression in *X. laevis* oocytes. Expression of PIP2;1 alone conferred, with respect to native oocytes, an 8-fold increase in cell osmotic water permeability ( $P_f$ ) (supplemental Fig. S4A, S4B). Coexpression of PIP2;1 with RKL1 and not with RLK902 resulted in a further increase in  $P_f$  by 50% (Fig. 4A, 4B, supplemental Fig. S4A, S4B). Three phosphorylation sites have been described in PIP2;1, at Ser<sup>121</sup>, Ser<sup>280</sup>, and Ser<sup>283</sup> (1, 4, 8). The  $P_f$  of oocytes expressing a PIP2;1 form with Ser-to-Ala mutations at positions 280 and 283 (Ser<sup>280</sup>Ala-Ser<sup>283</sup>Ala) was almost similar to  $P_f$  of oocytes expressing wild-type PIP2;1 (Fig. 4A, 4B). In addition, coexpression of RKL1 with PIP2;1 Ser<sup>280</sup>Ala-Ser<sup>283</sup>Ala resulted in a similar stimulation of  $P_f$  as with wild-type PIP2;1 (supplemental Fig. S4A). These results suggest that phosphorylation of PIP2;1 at Ser<sup>280</sup> and Ser<sup>283</sup>

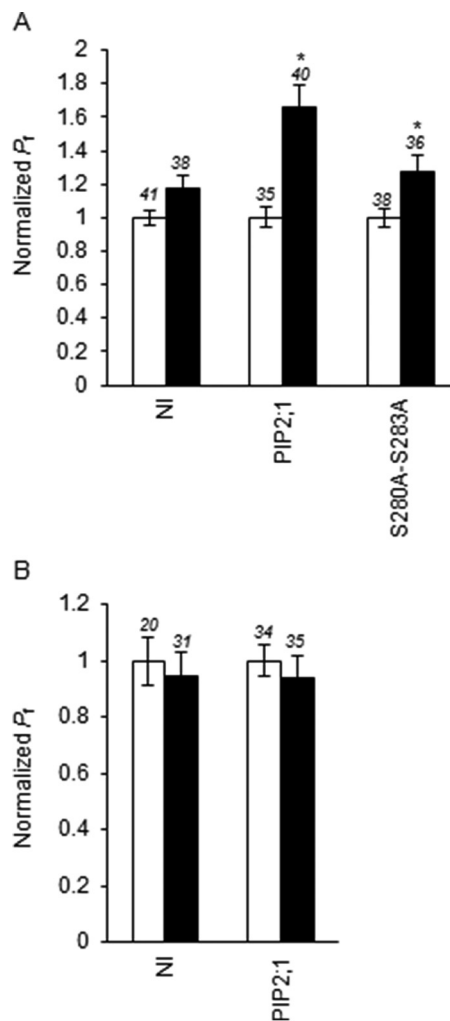


**Fig. 4. Functional co-expression in *Xenopus* Oocytes of PIP2;1 with RKL1 or RLK902.** NI: uninjected oocytes (white) and oocytes expressing RKL1 or RLK902 individually (black) were used as negative controls for oocytes expressing PIP2;1, alone or with the corresponding PK, respectively. Oocytes were injected with 1 to 3 ng of cRNAs encoding wild-type PIP2;1 or mutated PIP2;1 Ser<sup>280</sup>Ala-Ser<sup>283</sup>Ala (S280A-S283A), in the absence (white) and in the presence of 6 time more ng cRNAs encoding RKL1 (A) and RLK902 (B) (black). Oocyte osmotic water permeability ( $P_f$ ) was measured as described in the Experimental procedures and was normalized with regard to the  $P_f$  obtained in the absence of the enzyme. Asterisks indicate significant effects of PK on  $P_f$  (one-way ANOVA; Newman-Keuls,  $p$  value  $< 0.05$ ). Representative experiments are shown in supplemental Fig. S4A, S4B.

does not contribute to PIP2;1 activity in oocytes, and, in particular, to its enhancement upon coexpression with RKL1. One hypothesis is that Ser<sup>121</sup>, a residue described to be involved in aquaporin gating could be the target of RKL1. However punctual mutations of Ser<sup>121</sup>, to an Ala or Asp residue, led to inactive PIP2;1, thereby preventing to test this hypothesis.

By contrast to RKL1, coexpression of PIP2;1 with Feronia resulted, with respect to oocytes expressing PIP2;1 alone, in

TABLE I

Numerical analysis of FRET interactions between PIP2;1 and PIP2;1 interactants measured by FLIM. Average lifetimes of GFP fusion proteins expressed alone or together with mCherry-tagged or mRFP-tagged PIP2;1 and corresponding S.E. *N* and *n* correspond to the number of independent experiments and cells measured, respectively. *Annexin4*: At2g38750; *HIR3*: At3g01290; *RKL1*: At1g48480; *RLK902*: At3g17840; *Feronia*: At3g51550; *PLD $\delta$* : At4g35790; *PLD $\gamma$ 1*: At4g11850; *NHL3*: At5g06320

Donor	Acceptor	$\tau$ (ps) $\pm$ S.E.	FRET efficiency	<i>N/n</i>	<i>p</i> (t-test)
PIP2;1-GFP	-	2320 $\pm$ 7	-	3/17	-
PIP2;1-GFP	PIP2;1-mCherry	1851 $\pm$ 27	20%	1/9	3.21 $\times 10^{-17}$
PIP2;1-GFP	PIP2;1-RFP	1604 $\pm$ 70	31%	1/3	6.88 $\times 10^{-15}$
PIP2;1-GFP	RFP	2319 $\pm$ 19	0%	2/8	0.94
HIR3-GFP	-	2373 $\pm$ 20	-	3/12	-
HIR3-GFP	PIP2;1-RFP	2369 $\pm$ 20	0%	3/12	0.89
GFP-Annexin4	-	2387 $\pm$ 37	-	1/2	-
GFP-Annexin4 <sup>a</sup>	PIP2;1-mCherry	2436 $\pm$ 20	-2%	1/2	0.37
RKL1-GFP	-	2429 $\pm$ 7	-	3/20	-
RKL1-GFP	PIP2;1-mCherry	2261 $\pm$ 23	7%	3/20	2.59 $\times 10^{-8}$
RLK902-GFP	-	2390 $\pm$ 7	-	3/20	-
RLK902-GFP	PIP2;1-RFP	2209 $\pm$ 23	8%	3/20	4.88 $\times 10^{-9}$
Feronia-GFP	-	2385 $\pm$ 8	-	3/19	-
Feronia-GFP	PIP2;1-RFP	2121 $\pm$ 50	11%	3/20	9.92 $\times 10^{-6}$
GFP-NHL3	-	2396 $\pm$ 7	-	3/19	-
GFP-NHL3	PIP2;1-RFP	2085 $\pm$ 78	13%	3/16	1.33 $\times 10^{-4}$
PLD $\delta$ -GFP	-	2319 $\pm$ 13	-	2/8	-
PLD $\delta$ -GFP	PIP2;1-RFP	1946 $\pm$ 49	16%	2/7	2.97 $\times 10^{-6}$
PLD $\gamma$ 1-GFP	-	2390 $\pm$ 12	-	3/13	-
PLD $\gamma$ 1-GFP	PIP2;1-RFP	2075 $\pm$ 36	13%	3/13	1.39 $\times 10^{-8}$

<sup>a</sup> The interaction between GFP-PIP2;1 and mCherry-Annexin4 gave similar results as the interaction between GFP-Annexin4 and PIP2;1-mCherry (data not shown).

a decrease in  $P_f$  by 60% (Fig. 5). Lys<sup>565</sup> is a residue located in the catalytic domain of Feronia. Punctual mutation of Lys<sup>565</sup> to an Arg (Lys<sup>565</sup>Arg), or deletion of the C terminus of Feronia were shown to abolish its kinase activity (65). When coexpressed with PIP2;1, these mutated forms of Feronia failed to interfere with the water transport activity of the aquaporin (Fig. 5A). These results suggest that Feronia inhibits PIP2;1-mediated water transport through its PK activity. To investigate PIP2;1 residues that would be targeted by Feronia, we coexpressed the latter with forms of PIP2;1 carrying individual or combined mutations of Ser<sup>280</sup> and Ser<sup>283</sup> to Ala or Asp (Fig. 5B, supplemental Fig. S5). For all PIP2;1 forms carrying individual mutations, coexpression with Feronia resulted in a decrease in  $P_f$  by 15% to 38%, whereas wild-type PIP2;1 showed an inhibition by 45%. In addition, Feronia did not alter the  $P_f$  of oocytes expressing a Ser<sup>280</sup>Ala-Ser<sup>283</sup>Ala form of PIP2;1 whereas the Ser<sup>280</sup>Asp-Ser<sup>283</sup>Asp form showed a residual inhibition (Fig. 5B). These results indicate that Feronia possibly acts through Ser<sup>280</sup> and Ser<sup>283</sup>, but not exclusively through one of these residues. Furthermore, phosphodeficient mutations of both Ser<sup>280</sup> and Ser<sup>283</sup> appeared to fully prevent the inhibitory effect of Feronia whereas phosphomimetic mutations would allow partial inhibition.

**Functional Interaction Between Feronia and PIP2;1**—We then tested the hypothesis that phosphorylation at the C terminus of PIP2;1 could by itself favor interaction of Feronia with PIP2;1. FLIM analyses were performed in leaf epidermal cells that transiently expressed Feronia-GFP alone and in

combination with RFP-PIP2;1, either wild-type or with Ser<sup>280</sup> and Ser<sup>283</sup> mutations to Ala (PIP2;1 Ser<sup>280</sup>Ala-Ser<sup>283</sup>Ala) or Asp (PIP2;1 Ser<sup>280</sup>Asp-Ser<sup>283</sup>Asp) (Table II, Fig. 6). The WT and all mutated forms significantly interacted with Feronia. A statistical analysis revealed, however, that interactions between Feronia and the wild-type or Ser<sup>280</sup>Ala-Ser<sup>283</sup>Ala forms of PIP2;1 were weaker (*p* value 0.391) than the interaction between Feronia and the Ser<sup>280</sup>Asp-Ser<sup>283</sup>Asp form (*p* value 0.039). These results suggest that interaction of Feronia with PIP2;1 can occur, independent of its inhibitory effects and that the PK would preferentially interact with the phosphorylated form of PIP2;1.

## DISCUSSION

**PIP Interactome: A Platform Regrouping a Wide Range of Transport Activities**—PIP1;2 and PIP2;1, which are among the most highly expressed PIPs in both roots and leaves (66), bring a major contribution to root water transport and its regulation by hormonal and abiotic factors (67, 68). The objective of this work was to increase our knowledge of proteins that molecularly and functionally interact with PIP1;2 and PIP2;1 to get new insights into regulatory mechanisms of root water transport. For that, we used plants overexpressing PIP1;2 and PIP2;1 fused to GFP. These plants do not exhibit any particular growth phenotype when compared with wild-type plants. Such constructs were also shown to be functionally relevant ones across several studies: these constructs were used to show that stimulus-induced downregulation of

**FIG. 5. Functional co-expression in *Xenopus* Oocytes of PIP2;1 with Feronia.** A, Negative controls were obtained from uninjected oocytes (NI) and oocytes expressing either wild-type form of Feronia (FER-WT) or mutated form of Feronia with a Lys<sup>565</sup>Arg mutation (FER-K565R) or a C-terminal deletion (FER-Δ500). Oocytes were injected with 2.5 ng of cRNAs encoding PIP2;1 and, when indicated, were also injected with 15 ng of cRNA encoding FER-WT, FER-K565R or FER-Δ500. Data were normalized with regard to the  $P_f$  obtained with wild-type PIP2;1. B, Oocytes were uninjected (NI) or injected with 2.5 ng of cRNAs encoding wild-type PIP2;1 or mutated PIP2;1 Ser<sub>280</sub>Ala (S280A), Ser<sub>280</sub>Asp (S280D), Ser<sub>283</sub>Ala (S283A), Ser<sub>283</sub>Asp (S283D), Ser<sub>280</sub>Ala- Ser<sub>283</sub>Ala (S280A-S283A), Ser<sub>280</sub>Asp- Ser<sub>283</sub>Asp (S280D-S283D), in the absence (white) and in the presence of 15 ng cRNAs encoding Feronia (black). Data were normalized with regard to the  $P_f$  obtained in the absence of Feronia. A representative experiment is shown in [supplemental Fig. S5](#). Numbers indicate the number of oocytes.

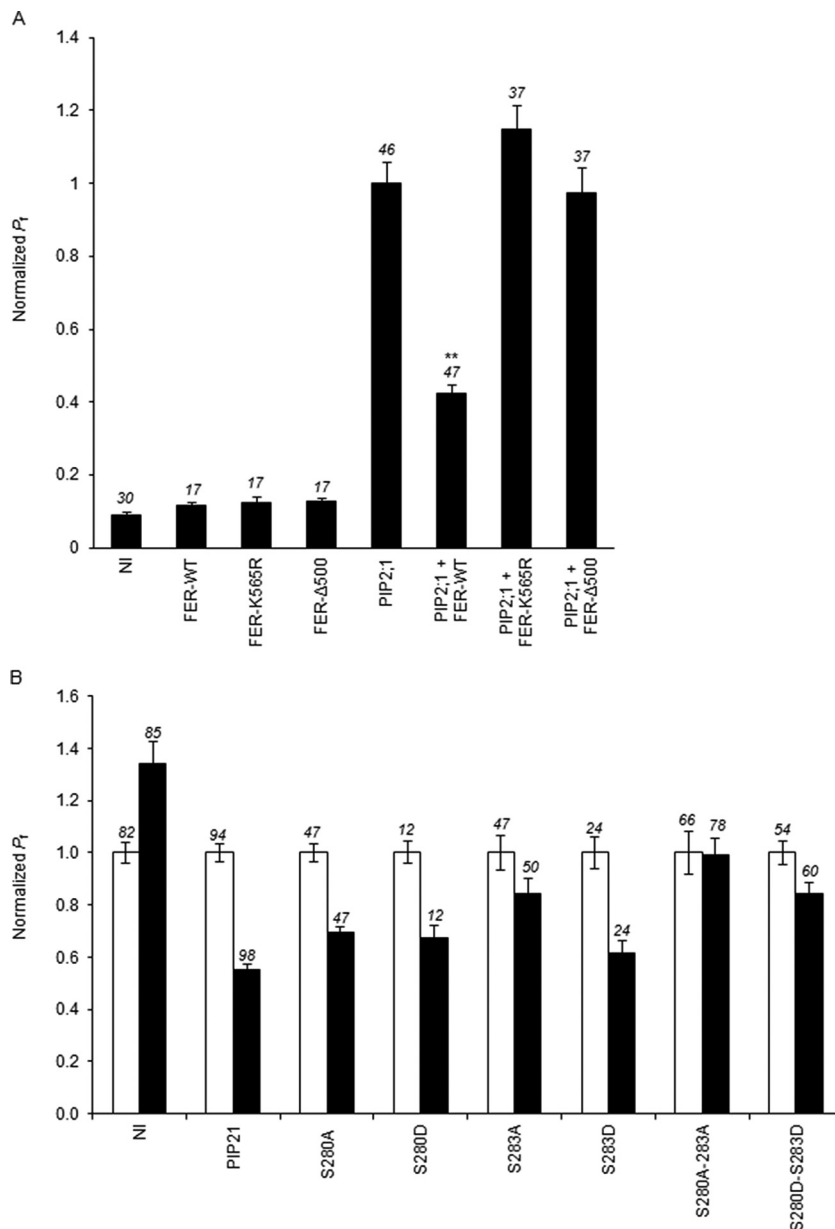


TABLE II

Characterization of FRET interaction between Feronia and PIP2;1. Average lifetimes of GFP fusion proteins expressed alone or together with mRFP-tagged PIP2;1 and corresponding S.E. PIP2;1 was either wild-type (WT) or with double punctual mutations of Ser280 and Ser283 in Ala (PIP2;1-AA) or in Asp (PIP2;1-DD). N and n correspond to the number of independent experiments and cells measured respectively

Donor	Acceptor	$\tau$ (ps) $\pm$ S.E.	FRET efficiency	N/n	p (t-test)
Feronia-GFP	-	2395 $\pm$ 6	-	4/19	-
Feronia-GFP	RFP-PIP2;1-WT	2276 $\pm$ 11	5%	4/17	2,10 $\times 10^{-11}$
Feronia-GFP	RFP-PIP2;1-AA	2288 $\pm$ 10	4%	4/21	9,31 $\times 10^{-11}$
Feronia-GFP	RFP-PIP2;1-DD	2227 $\pm$ 19	7%	4/19	8,45 $\times 10^{-10}$
Feronia-GFP	RFP	2418 $\pm$ 19	-1%	1/5	0,12

root water transport involves reactive oxygen species-activated cell signaling and PIP internalization (45). Another study, revealed, using these constructs, that endoplasmic reticulum-retained PIP2;1-GFP may interact with other PIP aquaporins

to hamper their trafficking to the plasma membrane, contributing to inhibition of root cell hydraulic conductivity (69). Finally, the use of these constructs for single-molecule analysis of PIP2;1 dynamics and membrane partitioning allowed to

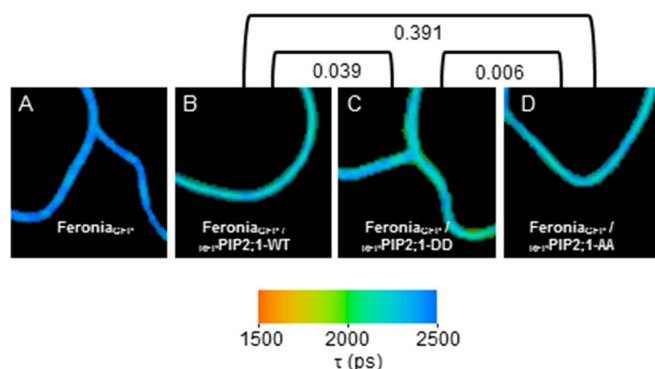


**FIG. 6. Physical interaction between phosphorylated forms of PIP2;1 and Feronia.** FLIM analyses were performed in leaf epidermal cells transiently expressing Feronia-GFP alone (A) and in combination with RFP-tagged PIP2;1 (B to D). The physical interaction between Feronia and PIP2;1 in its native form (PIP2;1-WT, B) and carrying double punctual mutations of Ser<sup>280</sup> and Ser<sup>283</sup> to Asp (PIP2;1-DD, C) or Ala (PIP2;1-AA, D) is shown. FRET values are indicated in Table II. *t* test performed between experiments and *p* values are indicated.

reveal multiple modes of aquaporin regulation (70). Such transgenic plants are thus relevant for PIP interactomic studies. A wide range of methods for tracking protein-protein interactions, whether based on biophysical, biochemical, computational, or genetic principles, have been developed for soluble proteins but are sometimes hardly suitable for membrane protein targets. To circumvent this problem, we used a buffer made of lowly concentrated detergents, allowing the extraction of membrane proteins with reduced dissociation of interactants from the membrane bait. In addition, we used formaldehyde-mediated protein cross-linking that recently emerged as an additional means for preserving cellular protein interactions while being compatible with numerous purification strategies (reviewed in (71)). An intrinsic complication of IP-MS is that it may give rise to false hits, in particular when using recombinant fusion proteins as a bait. In the present work, a plant line overexpressing GFP was used to discard interactions of unwanted proteins with GFP. A high number of putative PIP interactants still remained, even after using this control. Reverse IPs were performed to validate the initial IP approach. In brief, we selected three putative PIP1;2 or PIP2;1 interactants based on the availability of plants expressing GFP-fused proteins. Using plants expressing PGP4, PGP19, or AMT1;3 fused to GFP, we were able to pull down PIP1;2 and PIP2;1, thereby validating the IP-MS strategy (supplemental Table S6).

Surprisingly, more than 85% of identified interactants were shared by the PIP2;1 and PIP1;2 interactomes. One reason for this result may be that the two baits themselves interact with one another. Although their existence remains to be formally demonstrated, heterotetramers formed with distinct PIP homologs have been suggested from functional coexpression in *Xenopus* oocytes or yeast, or by FRET-based cellular imaging (24, 72, 73). Our analyses confirmed that PIP1;2 and PIP2;1

mutually interact. Thus, the high similarity between PIP1;2 and PIP2;1 interactomes may reflect a *in vivo* physical assembly between PIP1;2 and PIP2;1. Because the two aquaporins have similar functions, it is also not surprising that they share similar protein partners. Finally, because of the high number of identified PIP interactants, the present work constitutes the first thorough PIP interactome. This may be because of the use of *in vivo* crosslinking strategy that allowed to identify indirect and physical interactants of PIPs.

Because of their high complexity, the two PIP interactomes were then analyzed through sequential bioinformatical steps. These included a classification of interactants according to their molecular function, an analysis of enrichment in GO terms, and a network clustering study. The two first steps pointed to four characteristic molecular functions (Fig. 1B), mainly including transport and catalytic activities. A large body of evidence supports the existence of membrane microdomains in plants, in as diverse contexts as cell-to-cell interactions, stress, polarized growth, and membrane transport (74). Interestingly, more than 20% of PIP interactants have been described as enriched in microdomains (supplemental Table S3) although 33% have a transmembrane transport activity (not shown). Under resting conditions, PIP2;1 shows constitutive cycling from the plasma membrane *via* clathrin-mediated endocytosis, whereas under salt stress conditions, the protein follows an additional clathrin-independent internalization route (70), which is associated with flotillins, a marker of membrane microdomains (75). Thus, the PIP interactome may highlight a partitioning of aquaporins in several types of microdomains to ensure transport activities or trafficking at specific submembrane locations.

A network clustering procedure also revealed molecular functions that appear to be tightly connected to PIPs. These include the exocyst complex, in relation to the trafficking processes, BR signaling and GTPases. BR may control aquaporin activity (76) and induce genes involved in water transport, cell-wall organization, and biogenesis in relation to root cell elongation (77). Another link is H<sub>2</sub>O<sub>2</sub>, which inhibits aquaporin activity (45) and the production of which seems to be critical for BR-induced stress tolerance in plants (78–81). In the present work, we showed that the abundance of one component of BR cluster (At3g09840) in the PIP interactome was decreased upon H<sub>2</sub>O<sub>2</sub> treatment (supplemental Table S3). In addition, the hormonal network related to auxin and BRs appeared to be affected by PIP downregulation in poplar leaf (82). Thus, we hypothesize that BR signaling pathways could be linked to regulation of PIP function in roots.

**Regulation of PIP Trafficking**—Osmotic stresses induce a partial internalization of PIPs (34, 83) leading to a reduced abundance of PIPs at the root cell surface, which may contribute to a decrease of root water permeability. In addition, stimulus-induced PIP trafficking can be counteracted by reactive oxygen species (ROS) scavengers, in agreement with the central role played by ROS in stress and hormonal signal-

ing in plants (83). Thus, deciphering the molecular and cellular mechanisms that govern PIP dynamics is central to understand the perception and transduction of stress signals in plants. Syntaxins are among the few proteins known to be involved in PIP trafficking (25, 84). In particular, post-Golgi trafficking of *Arabidopsis* PIP2;7 was shown to depend on a physical interaction with two specific syntaxins, SYP61 and SYP121 (26). As mentioned above, clathrin-dependent and -independent endocytic mechanisms allow PIPs to cycle between the plasma membrane and early endosomes under resting conditions and osmotic or oxidative stresses, respectively (35, 70). The latter stresses also induce quantitative changes in the double C-terminal phosphorylation (Ser<sup>280</sup> and Ser<sup>283</sup>) of AtPIP2;1 (1, 8) whereas phosphorylation of Ser<sup>283</sup> interferes with trafficking of internalized PIPs to spherical bodies (8). In the present work, quantitative analysis of PIP interactome revealed that H<sub>2</sub>O<sub>2</sub> and NaCl treatments preferentially modify the abundance of interactants involved in vesicle-mediated trafficking (supplemental Table S9). These results support the previously described role of proteins such as syntaxins and clathrin in aquaporin regulation and point to additional protein partners acting on PIP trafficking.

**A Role for Lipid Signaling in PIP Function**—IP-MS studies do not allow to distinguish between proteins that physically or indirectly interact with the bait. With the objective of focusing on physical PIP interactants, we applied the FLIM technology to eight PIP interactants selected according to their molecular function, their quantitative variations according to H<sub>2</sub>O<sub>2</sub> and NaCl treatments, their putative enrichment in microdomains or their presence in a specific cluster. Among them, Annexin4 and HIR3 did not show any physical interaction with PIP2;1 (Fig. 3, Table I). By contrast, members of phospholipase D and RLK families as well as NHL3 showed a physical interaction with PIP2;1. Multiple lines of evidence indicate that, in humans, Aquaporin-3 (AQP3) and phospholipase D both contribute to skin function. AQP3 co-localizes with phospholipase D2 in caveolin-rich membrane micro-domains, the former delivering glycerol to the latter, for synthesis of phosphatidylglycerol, a lipid messenger regulating keratinocyte proliferation and differentiation (85). In plants, PLDs and their enzymatic product phosphatidic acid (PA) play roles in cellular responses to hormonal and abiotic stimuli, as well as in plant-microbial interactions and plant defense against bacterial and fungal pathogens (62). PA is therefore regarded as a universal lipid signaling molecule. It often directly binds to proteins to alter their localization, enzymatic activity, or interactions with membrane or cytoskeleton (86). More than 30 plant proteins from diverse physiological pathways have been identified as PA targets and the list is still being extended (62, for review). In particular, a recent work identified AtPIP2;1 and AtPIP2;2 as PA-binding (87) but the functional effects of these interactions remain to be elucidated. Additionally, AtPLD $\delta$  is required for ABA-induced stomatal closure, acting downstream of H<sub>2</sub>O<sub>2</sub> and nitric oxide in the ABA signaling pathway (88). Here,

we showed that, in roots, the quantity of PLD $\delta$  in the PIP2;1 and PIP1;2 interactome decreased upon H<sub>2</sub>O<sub>2</sub> treatment (supplemental Table S3). Thus, we hypothesize that a reduced physical interaction between PLD $\delta$  and PIP2;1 upon H<sub>2</sub>O<sub>2</sub> treatment would result in a decreased PA binding to PIP2;1, thereby altering PIP2;1 function. Such a role for lipid signaling in PIP2;1 function is consistent with the suggested role of lipid-mediated signaling in the transduction of stress signals arising from the soil (89).

**Differential Roles of Receptor-like Kinases in PIP Function**—The PKs known to act on PIPs include two PKs phosphorylating spinach SoPIP2;1 at Ser<sup>115</sup> and Ser<sup>274</sup> (9), OST1/SnRK2.6, a PK involved in guard cell ABA signaling (10), SIRK1 and BSK8, (12, 13). Our IP-MS strategy identified 37 kinases as putative PIP interactants, of which 16 are RLKs. RKL1 and RLK902 physically interact with PIP2;1 and both belong to the LRR III subfamily. RLK902 and RKL1 were described as functional PKs able to auto-phosphorylate (57). At the macroscopic level and in standard culture conditions, neither the *rlk1* and *rlk902* mutant lines nor the *rlk1/rlk902* double knockout line showed any significant phenotypes (57). Coexpression of PIP2;1 with RKL1 in oocytes enhanced PIP2;1 water transport activity (Fig. 4A). However, despite a 75% amino acid sequence identity with RKL1, RLK902 was unable to activate PIP2;1 water transport activity (Fig. 4B), suggesting a strong specificity of these two PKs toward their substrates. Previous structure-function analyses have revealed the role of several cytosol-exposed phosphorylation sites of PIPs in controlling their water transport activity (21). In our study, PIP2;1 mutant analysis showed that stimulation by RKL1 is not mediated through two well-characterized C-terminal phosphorylation sites, Ser<sup>280</sup> and Ser<sup>283</sup>. Because a recent study showed that Ser<sup>121</sup> of loop B is the target of OST1/SnRK2.6 (10) we also investigated punctual mutations at this site. However, none of the mutated forms (Ser<sup>121</sup>Ala, Ser<sup>121</sup>Asp) yielded an active PIP2;1. Thus, in the absence of direct biochemical evidence, we cannot definitely conclude about the phosphorylation site(s) recognized by RKL1 in PIP2;1.

By contrast to RKL1, co-expression of PIP2;1 with *Feronia* decreased PIP2;1 water transport activity by 60% (Fig. 5). *Feronia* belongs to the *Catharanthus roseus* RLK1-like kinase family (CrRLK1Ls) characterized by their extracellular carbohydrate-binding lectin domains (90). Several recent works demonstrated that *Feronia* is critical to fine-tuning cell growth. In particular, it controls apoplastic pH (58) and ROS (59, 60), thereby balancing wall rigidity for cell integrity and flexibility during cell expansion. A recent study demonstrated that, upon binding to a small secreted peptide, RAPID ALKALIZATION FACTOR (RALF) (58), *Feronia* acts as a growth inhibitor in the root post-elongation zone. In the present work, punctual mutation of the kinase domain of *Feronia* or its deletion prevented the inhibitory effect of *Feronia* on PIP2;1 (Fig. 5) demonstrating that this effect is mediated through phosphor-

ylation. Functional analysis of PIP2;1 punctual mutants showed that inhibitory effect of Feronia was not individually mediated through Ser<sup>280</sup> or Ser<sup>283</sup> (Fig. 5). By contrast, a double phospho-deficient form (Ser<sup>280</sup>Ala-Ser<sup>283</sup>Ala) but not a double phospho-mimetic form (Ser<sup>280</sup>Asp-Ser<sup>283</sup>Asp) of PIP2;1 had become resistant to the inhibitory effect of Feronia (Fig. 5B). Thus, the combined phosphorylation of these two sites may favor the inhibitory action of Feronia. We do not believe that Ser<sup>280</sup> and Ser<sup>283</sup> serve as phosphorylation sites for Feronia. We rather showed that binding of Feronia to PIP2;1 may be favored by their combined phosphorylation (Fig. 6, Table II). Because phosphorylation of both Ser<sup>280</sup> and Ser<sup>283</sup> is supposed to lead to PIP2;1 activation, the mechanism by which Feronia inhibits aquaporin activity remains unknown. Once it is bound to PIP2;1 C-terminal tail, Feronia may phosphorylate its partner at an unknown site, that would in turn inhibit PIP2;1 activity. Alternatively, Feronia binding to PIP2;1 may favor the recruitment and/or phosphorylation of a protein phosphatase that would dephosphorylate PIP2;1, thereby reducing its activity. These hypotheses deserve additional experiments.

*In conclusion*, the present work provides the most complete interactome of PIPs so far described in plant. It reveals that PIPs behave as a platform for recruitment of a wide range of transport activities. The work also brings additional insights into the regulation of PIP cellular trafficking by osmotic and oxidative treatments. Finally, it pinpoints a role for lipid signaling in PIP function and enhances our knowledge of PKs involved in PIP regulation. In particular, we show that two members of the RLK family differentially modulate PIP function, although the molecular mechanisms involved still deserve additional experiments. The overall work opens novel perspectives in understanding mechanisms involved in PIP regulation and adjustment of plant water status.

*Acknowledgments*—We thank the Mass Spectrometry Proteomics Platform (MSPP) for its technical support regarding proteomics experiments, Carine Alcon and Sylvain Rossi for their technical help in FLIM measurements performed on MRI (Montpellier Rio Imaging platform, Montpellier), Cécile Fizames and Olivier Langella for bioinformatical assistance.

\* This work was supported by a research contract with Syngenta.

§ This article contains [supplemental material](#).

§ To whom correspondence should be addressed: Biochimie et Physiologie Moléculaire des Plantes, INRA, 2 place Viala, Montpellier 34060 France. Tel.: 33-4-99 61 20 20; E-mail: [santoniv@supagro.inra.fr](mailto:santoniv@supagro.inra.fr).

#### REFERENCES

- Di Pietro, M., Vialaret, J., Li G-W, Hem, S., Prado, K., Rossignol, M., Maurel, C., and Santoni, V. (2013) Coordinated post-translational responses of aquaporins to abiotic and nutritional stimuli in *Arabidopsis* roots. *Mol. Cell. Proteomics* **12**, 3886–3897
- Maurel, C., Verdoucq, L., Luu D-T, and Santoni, V. (2008) Plant aquaporins: membrane channels with multiple integrated functions. *Annu. Rev. Plant Biol.* **59**, 595–624
- Kaldenhoff, R., Ribas-Carbo, M., Flexas, J., Lovisolo, C., Heckwolf, M., and Uehlein, N. (2008) Aquaporins and plant water balance. *Plant Cell Environ.* **31**, 658–666
- Tomroth-Horsefield, S., Wang, Y., Hedfalk, K., Johanson, U., Karlsson, M., Tajkhorshid, E., Neutze, R., and Kjellbom, P. (2006) Structural mechanism of plant aquaporin gating. *Nature* **439**, 688–694
- Johanson, U., and Gustavsson, S. (2002) A new subfamily of major intrinsic proteins in plants. *Mol. Biol. Evol.* **19**, 456–461
- Quigley, F., Rosenberg, J. M., Shachar-Hill, Y., and Bohnert, H. J. (2002) From genome to function: the *Arabidopsis* aquaporins. *Genome Biol.* **3**, 1–17
- Ishikawa, F., Suga, S., Uemura, T., Sato, M. H., and Maeshima, M. (2005) Novel type aquaporins SIPs are mainly localized to the ER membrane and show cell-specific expression in *Arabidopsis thaliana*. *Febbs Let.* **579**, 5814–5820
- Prak, S., Hem, S., Boudet, J., Viennois, J., Sommerer, N., Rossignol, R., Maurel, C., and Santoni, V. (2008) Multiple phosphorylations in the C-terminal tail of plant plasma membrane aquaporins. Role in sub-cellular trafficking of AtPIP2;1 in response to salt stress. *Mol. Cell. Proteomics* **7**, 1019–1030
- Sjovall-Larsen, S., Alexandersson, E., Johansson, I., Karlsson, M., Johanson, U., and Kjellbom, P. (2006) Purification and characterization of two protein kinases acting on the aquaporin SoPIP2;1. *Biochim. Biophys. Acta* **1758**, 1157–1164
- Grondin, A., Rodrigues, O., Verdoucq, L., Merlot, S., Leonhardt, N., and Maurel, C. (2015) Aquaporins contribute to ABA-triggered stomatal closure through OST1-mediated phosphorylation. *Plant Cell* **27**, 1–11
- Morillo, S. A., and Tax, F. E. (2006) Functional analysis of receptor-like kinases in monocots and dicots. *Curr. Opin. Plant Biol.* **9**, 460–469
- Niittylä, T., Fuglsang, A. T., Palmgren, M. G., Frommer, W. B., and Schulze, W. X. (2007) Temporal analysis of sucrose-induced phosphorylation changes in plasma membrane proteins of *Arabidopsis*. *Mol. Cell. Proteomics* **6**, 1711–1726
- Wu, X. N., Sanchez-Rodriguez, C., Pertl-Obermeyer, H., Obermeyer, G., and Schulze, W. X. (2013) Sucrose-induced receptor kinase SIRK1 regulates plasma membrane aquaporins in *Arabidopsis*. *Mol. Cell. Proteomics* **12**, 2856–2873
- Wu, F. Q., Sheng, P. K., Tan, J. J., Chen, X. L., Lu, G. W., Ma, W. W., Heng, Y. Q., Lin, Q. B., Zhu, S. S., Wang, J. L., Wang, J., Guo, X. P., Zhang, X., Lei, C. L., and Wan, J. M. (2015) Plasma membrane receptor-like kinase leaf panicle 2 acts downstream of the drought and salt tolerance transcription factor to regulate drought sensitivity in rice. *J. Exp. Bot.* **66**, 271–281
- Chen, J., Lalonde, S., Obrdlik, P., Noorani Vatani, A., Parsa, S. A., Vilarino, C., Revuelta, J. L., Frommer, W. B., and Rhee, S. Y. (2012) Uncovering *Arabidopsis* membrane protein interactome enriched in transporters using mating-based split ubiquitin assays and classification models. *Front. Plant Sci.* **3**, 124
- Jones, A. M., Xuan, Y. H., Xu, M., Wang, R. S., Ho, C. H., Lalonde, S., You, C. H., Sardi, M. I., Parsa, S. A., Smith-Valle, E., Su, T. Y., Frazer, K. A., Pilot, G., Pratelli, R., Grossmann, G., Acharya, B. R., Hu, H. C., Engineer, C., Villiers, F., Ju, C. L., Takeda, K., Su, Z., Dong, Q. F., Assmann, S. M., Chen, J., Kwak, J. M., Schroeder, J. I., Albert, R., Rhee, S. Y., and Frommer, W. B. (2014) Border control - A membrane-linked interactome of *Arabidopsis*. *Science* **344**, 711–716
- Lalonde, S., Sero, A., Pratelli, R., Pilot, G., Chen, J., Sardi, M. I., Parsa, S. A., Kim, D. Y., Acharya, B. R., Stein, E. V., Hu, H. C., Villiers, F., Takeda, K., Yang, Y., Han, Y. S., et al. (2010) A membrane protein/signaling protein interaction network for *Arabidopsis* version AMPv2. *Front. Physiol.* **1**, 24
- Braun, P., Carvunis, A. R., Charlotiaux, B., Dreze, M., Ecker, J. R., Hill, D. E., Roth, F. P., Vidal, M., Galli, M., Balumuri, P., Bautista, V., Chesnut, J. D., Kim, R. C., de los Reyes, C., Gilles, P., Kim, C. J., Matrubutham, U., Mirchandani, J., Olivares, E., Patnaik, S., Quan, R., Ramaswamy, G., Shinn, P., Swamilingiah, G. M., Wu, S., Byrdsong, D., Dricot, A., Duarte, M., Gebreab, F., Gutierrez, B. J., MacWilliams, A., Monachello, D., Mukhtar, M. S., Poulin, M. M., Reichert, P., Romero, V., Tam, S., Waaijers, S., Weiner, E. M., Cusick, M. E., Tasan, M., Yazaki, J., Ahn, Y. Y., Barabasi, A. L., Chen, H. M., Dangl, J. L., Fan, C. Y., Gai, L. T., Ghoshal, G., Hao, T., Lurin, C., Milenkovic, T., Moore, J., Pevzner, S. J., Przulj, N., Rabello, S., Rietman, E. A., Rolland, T., Santhanam, B., Schmitz, R. J., Spooner, W., Stein, J., Vandenhaute, J., Ware, D., and Arabidopsis

- Interactome Mapping, C. (2011) Evidence for network evolution in an *Arabidopsis* interactome map. *Science* **333**, 601–607
19. Dedecker, M., Van Leene, J., and De Jaeger, G. (2015) Unravelling plant molecular machineries through affinity purification coupled to mass spectrometry. *Cur. Op. Plant Biol.* **24**, 1–9
  20. Marcilla, M., and Albar, J. P. (2013) Quantitative proteomics: A strategic ally to map protein interaction networks. *IUBMB Life* **65**, 9–16
  21. Maurel, C., Boursiac, Y., Luu D-T, Santoni, V., Shahzad, Z., and Verdoucq, L. (2015) Aquaporins in Plants. *Physiol. Rev.* **95**, 1321–1358
  22. Chen, W., Yin, X., Wang, L., Tian, J., Yang, R. Y., Liu, D. F., Yu, Z. H., Ma, N., and Gao, J. P. (2013) Involvement of rose aquaporin *RhPIP1;1* in ethylene-regulated petal expansion through interaction with *RhPIP2;1*. *Plant Mol. Biol.* **83**, 219–233
  23. Li, D. D., Ruan, X. M., Zhang, J., Wu, Y. J., Wang, X. L., and Li, X. B. (2013) Cotton plasma membrane intrinsic protein 2s (PIP2s) selectively interact to regulate their water channel activities and are required for fibre development. *New Phytol.* **199**, 695–707
  24. Zelazny, E., Borst, J. W., Muylaert, M., Batoko, H., Hemminga, M. A., and Chaumont, F. (2007) FRET imaging in living maize cells reveals that plasma membrane aquaporins interact to regulate their subcellular localization. *Proc. Natl. Acad. Sci. U.S.A.* **104**, 12359–12364
  25. Besserer, A., Burnotte, E., Bienert, G. P., Chevalier, A. S., Errachid, A., Grefen, C., Blatt, M. R., and Chaumont, F. (2012) Selective Regulation of Maize Plasma Membrane Aquaporin Trafficking and Activity by the SNARE SYP121. *Plant Cell* **24**, 3463–3481
  26. Hachez, C., Laloux, T., Reinhardt, H., Cavez, D., Degand, H., Grefen, C., De Rycke, R., Inze, D., Blatt, M. R., Russinova, E., and Chaumont, F. (2014) *Arabidopsis* SNAREs SYP61 and SYP121 coordinate the trafficking of plasma membrane aquaporin PIP2;7 to modulate the cell membrane water permeability. *Plant Cell* **26**, 3132–3147
  27. Hachez, C., Veljanovski, V., Reinhardt, H., Guillaumot, D., Vanhee, C., Chaumont, F., and Batoko, H. (2014) The *Arabidopsis* abiotic stress-induced TSP0-related protein reduces cell-surface expression of the aquaporin PIP2;7 through protein-protein interactions and autophagic degradation. *Plant Cell* **26**, 4974–4990
  28. Lee, H. K., Cho, S. K., Son, O., Xu, Z., Hwang, I., and Kim, W. T. (2009) Drought stress-induced Rma1H1, a RING membrane-anchor E3 ubiquitin ligase homolog, regulates aquaporin levels via ubiquitination in transgenic *Arabidopsis* plants. *Plant Cell* **21**, 622–641
  29. Cutler, S. R., Ehrhardt, D. W., Griffiths, J. S., and Sommerville, C. R. (2000) Random GFP::cDNA fusions enable visualization of subcellular structures in cells of *Arabidopsis* at a high frequency. *Proc. Natl. Acad. Sci. U.S.A.* **97**, 3718–3723
  30. Murashige, T., and Skoog, F. (1962) A revised medium for rapid growth and bioassays with tobacco tissue cultures. *Physiol. Plant.* **15**, 473–497
  31. Lima, J. E., Kojima, S., Takahashi, H., and von Wiren, N. (2010) Ammonium triggers lateral root branching in *Arabidopsis* in an ammonium transporter1;3-dependent manner. *Plant Cell* **22**, 3621–3633
  32. Cho, M., Lee, S. H., and Cho, H. T. (2007) P-glycoprotein4 displays auxin efflux transporter-like action in *Arabidopsis* root hair cells and tobacco cells. *Plant Cell* **19**, 3930–3943
  33. Lewis, D. R., Wu, G. S., Ljung, K., and Spalding, E. P. (2009) Auxin transport into cotyledons and cotyledon growth depend similarly on the ABCB19 multidrug resistance-like transporter. *Plant J.* **60**, 91–101
  34. Boursiac, Y., Chen, S., Luu D-T, Sorieul, M., van den Dries, N., and Maurel, C. (2005) Early effects of salinity on water transport in *Arabidopsis* roots. Molecular and cellular features of aquaporin expression. *Plant Physiol.* **139**, 790–805
  35. Wudick, M. M., Li, X., Valentini, V., Geldner, N., Chory, J., Lin, J., Maurel, C., and Doan-Trung, L. (2015) Subcellular redistribution of root aquaporins induced by hydrogen peroxide. *Mol. Plant* **8**, 1103–1114
  36. Wicniewski, J. R., Zougman, A., Nagaraj, N., and Mann, M. (2009) Universal sample preparation method for proteome analysis. *Nat. Methods* **6**, 359–362
  37. Valot, B., Langella, O., Nano, E., and Zivy, M. (2011) MassChroQ: A versatile tool for mass spectrometry quantification. *Proteomics* **11**, 3572–3577
  38. Langella, O., Valot, B., Jacob, D., Balliau, T., Flores, R., Hoogland, C., Joets, J., and Zivy, M. (2013) Management and dissemination of MS proteomic data with PROTiCdb: Example of a quantitative comparison between methods of protein extraction. *Proteomics* **13**, 1457–1466
  39. Mi, H. Y., Muruganujan, A., Casagrande, J. T., and Thomas, P. D. (2013) Large-scale gene function analysis with the PANTHER classification system. *Nat. Protoc.* **8**, 1551–1566
  40. Shannon, P., Markiel, A., Ozier, O., Baliga, N. S., Wang, J. T., Ramage, D., Amin, N., Schwikowski, B., and Ideker, T. (2003) Cytoscape: A software environment for integrated models of biomolecular interaction networks. *Genome Res.* **13**, 2498–2504
  41. Bader, G. D., and Hogue, C. W. (2003) An automated method for finding molecular complexes in large protein interaction networks. *BMC Bioinformatics* **4**, 2
  42. Sparkes, I. A., Runions, J., Kearns, A., and Hawes, C. (2006) Rapid, transient expression of fluorescent fusion proteins in tobacco plants and generation of stably transformed plants. *Nat. Protoc.* **1**, 2019–2025
  43. Ameer-Beg, S. M., Edme, N., Peter, M., Barber, P. R., Ng, T., and Vojnovic, B. (2003) Imaging protein-protein interactions by multiphoton FLIM. In *Confocal, Multiphoton, and Nonlinear Microscopic Imaging* (Wilson, T., ed) Vol. 5139 pp. 180–189, Spie-Int Soc Optical Engineering, Bellingham
  44. Maurel, C., Reizer, J., Schroeder, J. I., and Chrispeels, M. J. (1993) The vacuolar membrane protein g-TIP creates water specific channels in *Xenopus* oocytes. *EMBO J.* **12**, 2241–2247
  45. Boursiac, Y., Boudet, J., Postaire, O., Luu D-T, Tournaire-Roux, C., and Maurel, C. (2008) Stimulus-induced down-regulation of root water transport involves reactive oxygen species cell signalling and plasma membrane intrinsic protein internalization. *Plant J.* **56**, 207–218
  46. Klockenbusch, C., and Kast, J. (2010) Optimization of formaldehyde cross-linking for protein interaction analysis of non-tagged Integrin beta 1. *J. Biomed. Biotech.* doi: 10.1155/2010/927585
  47. Wodak, S. J., Vlasblom, J., Turinsky, A. L., and Pu, S. Y. (2013) Protein-protein interaction networks: the puzzling riches. *Curr. Opin. Struct. Biol.* **23**, 941–953
  48. Loque, D., Yuan, L., Kojima, S., Gojon, A., Wirth, J., Gazzarrini, S., Ishiyama, K., Takahashi, H., and von Wiren, N. (2006) Additive contribution of AMT1;1 and AMT1;3 to high-affinity ammonium uptake across the plasma membrane of nitrogen-deficient *Arabidopsis* roots. *Plant J.* **48**, 522–534
  49. Rojas-Pierce, M., Titapiwatanakun, B., Sohn, E. J., Fang, F., Larive, C. K., Blakeslee, J., Cheng, Y., Cuttler, S., Peer, W. A., Murphy, A. S., and Raikhel, N. V. (2007) *Arabidopsis* P-glycoprotein19 participates in the inhibition of gravitropism by gravacin. *Chem. Biol.* **14**, 1366–1376
  50. Asama, K., and Sober, A. (2005) Seasonal courses of maximum hydraulic conductance in shoots of six temperate deciduous tree species. *Functional Plant Biol.* **32**, 1077–1087
  51. Keinath, N. F., Kierszniowska, S., Lorek, J., Bourdais, G., Kessler, S. A., Shimosato-Asano, H., Grossniklaus, U., Schulze, W. X., Robatzek, S., and Panstruga, R. (2010) PAMP (Pathogen-associated Molecular Pattern)-induced changes in plasma membrane compartmentalization reveal novel components of plant immunity. *J. Biol. Chem.* **285**, 39140–39149
  52. Kierszniowska, S., Seiwert, B., and Schulze, W. X. (2009) Definition of *Arabidopsis* sterol-rich membrane microdomains by differential treatment with methyl-beta-cyclodextrin and quantitative proteomics. *Mol. Cell. Proteomics* **8**, 612–623
  53. Minami, A., Fujiwara, M., Furuto, A., Fukao, Y., Yamashita, T., Kamo, M., Kawamura, Y., and Uemura, M. (2009) Alterations in detergent-resistant plasma membrane microdomains in *Arabidopsis thaliana* during cold acclimation. *Plant Cell Physiol.* **50**, 341–359
  54. Wu, H., Rossi, G., and Brennwald, P. (2008) The ghost in the machine: small GTPases as spatial regulators of exocytosis. *Trends Cell Biol.* **18**, 397–404
  55. Synek, L., Sekeres, J., and Zarsky, V. (2014) The exocyst at the interface between cytoskeleton and membranes in eukaryotic cells. *Front. Plant Sci.* **4**, 543
  56. Marshall, A., Aalen, R. B., Audenaert, D., Beeckman, T., Broadley, M. R., Butenko, M. A., Cano-Delgado, A. I., de Vries, S., Dresselhaus, T., Felix, G., Graham, N. S., Foulkes, J., Granier, C., Greb, T., Grossniklaus, U., Hammond, J. P., Heidstra, R., Hodgman, C., Hothorn, M., Inze, D., Ostergaard, L., Russinova, E., Simon, R., Skirycz, A., Stahl, Y., Zipfel, C., and De Meete, I. (2012) Tackling drought stress: receptor-like kinases present new approaches. *Plant Cell* **24**, 2262–2278
  57. Tarutani, Y., Sasaki, A., Yasuda, M., Nakashita, H., Yoshida, S., Yamaguchi, I., and Suzuki, Y. (2004) Identification of three clones which commonly interact with the kinase domains of highly homologous two receptor-like kinases, RLK902 and RKL1. *Biosci. Biotech. Biochem.* **68**, 2581–2587

58. Haruta, M., Sabat, G., Stecker, K., Minkoff, B. B., and Sussman, M. R. (2014) A peptide hormone and its receptor protein kinase regulate plant cell expansion. *Science* **343**, 408–411
59. Duan, Q. H., Kita, D., Johnson, E. A., Aggarwal, M., Gates, L., Wu, H. M., and Cheung, A. Y. (2014) Reactive oxygen species mediate pollen tube rupture to release sperm for fertilization in *Arabidopsis*. *Nature Com.* **5**
60. Duan, Q. H., Kita, D., Li, C., Cheung, A. Y., and Wu, H. M. (2010) FERONIA receptor-like kinase regulates RHO GTPase signaling of root hair development. *Proc. Nat. Acad. Sci. (U.S.A.)* **107**, 17821–17826
61. Wang, X. M., Devalah, S. P., Zhang, W. H., and Welti, R. (2006) Signaling functions of phosphatidic acid. *Prog. Lipid Res.* **45**, 250–278
62. Zhao, J. (2015) Phospholipase D and phosphatidic acid in plant defence response: from protein-protein and lipid-protein interactions to hormone signalling. *J. Exp. Bot.* **66**, 1721–1736
63. Rescher, U., and Gerke, V. (2004) Annexins - unique membrane binding proteins with diverse functions. *J. Cell Sci.* **117**, 2631–2639
64. Tamma, G., Procino, G., Mola, M. G., Svelto, M., and Valenti, G. (2008) Functional involvement of annexin-2 in cAMP induced AQP2 trafficking. *Pflugers Arch.* **456**, 729–736
65. Shih, H. W., Miller, N. D., Dai, C., Spalding, E. P., and Monshausen, G. B. (2014) The receptor-like kinase FERONIA is required for mechanical signal transduction in *Arabidopsis* seedlings. *Curr. Biol.* **24**, 1887–1892
66. Monneuse, J. M., Sugano, M., Becue, T., Santoni, V., Hem, S., and MR. (2011) Towards the profiling of the *Arabidopsis thaliana* plasma membrane transportome by targeted proteomics. *Proteomics* **11**, 1789–1797
67. Peret, B., Li, G. W., Zhao, J., Band, L. R., Voss, U., Postaire, O., Luu, D. T., Da Ines, O., Casimiro, I., Lucas, M., Wells, D. M., Lazzerini, L., Nacry, P., King, J. R., Jensen, O. E., Schaffner, A. R., Maurel, C., and Bennett, M. J. (2012) Auxin regulates aquaporin function to facilitate lateral root emergence. *Nat. Cell Biol.* **14**, 991–998
68. Postaire, O., Tournaire-Roux, C., Grondin, A., Boursiac, Y., Morillon, R., Schäffner, T., and Maurel, C. (2010) A PIP1 aquaporin contributes to hydrostatic pressure-induced water transport in both the root and rosette of *Arabidopsis*. *Plant Physiol.* **152**, 1418–1430
69. Sorieul, M., Santoni, V., Maurel, C., and Luu, D. T. (2011) Mechanisms and effects of retention of over-expressed aquaporin AtPIP2;1 in the endoplasmic reticulum. *Traffic* **12**, 473–482
70. Li, X. J., Wang, X. H., Yang, Y., Li, R. L., He, Q. H., Fang, X. H., Luu, D. T., Maurel, C., and Lin, J. X. (2011) Single-molecule analysis of PIP2;1 dynamics and partitioning reveals multiple modes of *Arabidopsis* plasma membrane aquaporin regulation. *Plant Cell* **23**, 3780–3797
71. Toews, J., Rogalski, J. C., Clark, T. J., and Kast, J. (2008) Mass spectrometric identification of formaldehyde-induced peptide modifications under in vivo protein cross-linking conditions. *Anal. Chim. Acta* **618**, 168–183
72. Fetter, K., Van Wilder, V., Moshelion, M., and Chaumont, F. (2004) Interactions between plasma membrane aquaporins modulate their water channel activity. *Plant Cell* **16**, 215–228
73. Temmei, Y., Uchida, S., Hoshino, D., Kanzawa, N., Kuwahara, M., Sasaki, S., and Tsuchiya, T. (2005) Water channel activities of *Mimosa pudica* plasma membrane intrinsic proteins are regulated by direct interaction and phosphorylation. *Febbs Let.* **579**, 4417–4422
74. Malinsky, J., Opekarova, M., Grossmann, G., and Tanner, W. (2013) Membrane Microdomains, Rafts, and Detergent-Resistant Membranes in Plants and Fungi. In *Annual Review of Plant Biology*, Vol 64 (Merchant, S. S., ed) Vol. 64 pp. 501–529, Annual Reviews, Palo Alto
75. Jarsch, I. K., Konrad, S. S. A., Stratil, T. F., Urbanus, S. L., Szymanski, W., Braun, P., Braun, K. H., and Ott, T. (2014) Plasma membranes are subcompartmentalized into a plethora of coexisting and diverse microdomains in *Arabidopsis* and *Nicotiana benthamiana*. *Plant Cell* **26**, 1698–1711
76. Morillon, R., Catterou, M., Sangwan, R. S., Sangwan, B. S., and Lassalles, J. P. (2001) Brassinolide may control aquaporin activities in *Arabidopsis thaliana*. *Planta* **212**, 199–204
77. Chaiwanon, J., and Wang, Z. Y. (2015) Spatiotemporal brassinosteroid signaling and antagonism with auxin pattern stem cell dynamics in *Arabidopsis* roots. *Curr. Biol.* **25**
78. Choudhary, S. P., Yu, J. Q., Yamaguchi-Shinozaki, K., Shinozaki, K., and Tran, L. S. P. (2012) Benefits of brassinosteroid crosstalk. *Trends Plant Sci.* **17**, 594–605
79. Xia, X. J., Wang, Y. J., Zhou, Y. H., Tao, Y., Mao, W. H., Shi, K., Asami, T., Chen, Z. X., and Yu, J. Q. (2009) Reactive oxygen species are involved in brassinosteroid-induced stress tolerance in cucumber. *Plant Physiol.* **150**, 801–814
80. Zhou, J., Wang, J., Li, X., Xia, X. J., Zhou, Y. H., Shi, K., Chen, Z. X., and Yu, J. Q. (2014) H<sub>2</sub>O<sub>2</sub> mediates the crosstalk of brassinosteroid and abscisic acid in tomato responses to heat and oxidative stresses. *J. Exp. Bot.* **65**, 4371–4383
81. Zhang, A., Zhang, J., Ye, N. H., Cao, J. M., Tan, M. P., Zhang, J. H., and Jiang, M. Y. (2010) ZmMPK5 is required for the NADPH oxidase-mediated self-propagation of apoplastic H<sub>2</sub>O<sub>2</sub> in brassinosteroid-induced antioxidant defence in leaves of maize. *J. Exp. Bot.* **61**, 4399–4411
82. Bi, Z., Merl-Pham, J., Uehlein, N., Zimmer, I., Mühlhans, S., Aichler, M., Walch, A. K., Kaldenhoff, R., Palme, K., Schnitzler, J. P., and Block, K. (2015) RNAi-mediated downregulation of poplar plasma membrane intrinsic proteins (PIPs) changes plasma membrane proteome composition and affects leaf physiology. *J. Proteomics* **128**, 321–332
83. Boursiac, Y., Prak, S., Boudet, J., Postaire, O., Luu D-T, Tournaire-Roux, C., Santoni, V., and Maurel, C. (2008) The response of *Arabidopsis* root water transport to a challenging environment implicates reactive oxygen species- and phosphorylation-dependent internalization of aquaporins. *Plant Sig. Behav.* **3**, 1096–1098
84. Tyrrell, M., Campanoni, P., Sutter, J. U., Pratelli, R., Paneque, M., Sokolovski, S., and Blatt, M. R. (2007) Selective targeting of plasma membrane and tonoplast traffic by inhibitory (dominant-negative) SNARE fragments. *Plant J.* **51**, 1099–1115
85. Qin, H. X., Zheng, X. J., Zhong, X. F., Shetty, A. K., Elias, P. M., and Bollag, W. B. (2011) Aquaporin-3 in keratinocytes and skin: Its role and interaction with phospholipase D2. *Arch. Biochem. Biophys.* **508**, 138–143
86. Testerink, C., and Munnik, T. (2011) Molecular, cellular, and physiological responses to phosphatidic acid formation in plants. *J. Exp. Bot.* **62**, 2349–2361
87. McLoughlin, F., Arisz, S. A., Dekker, H. L., Kramer, G., de Koster, C. G., Haring, M. A., Munnik, T., and Testerink, C. (2013) Identification of novel candidate phosphatidic acid-binding proteins involved in the salt-stress response of *Arabidopsis thaliana* roots. *Biochem. J.* **451**, 343–343
88. Distefano, A. M., Scuffi, D., Garcia-Mata, C., Lamattina, L., and Laxalt, A. M. (2012) Phospholipase D delta is involved in nitric oxide-induced stomatal closure. *Planta* **236**, 1899–1907
89. Vialaret, J., Di Pietro, M., Hem, S., Maurel, C., Rossignol, M., and Santoni, V. (2014) Phosphorylation dynamics of membrane proteins from *Arabidopsis* roots submitted to salt stress. *Proteomics* **14**, 1058–1070
90. Escobar-Restrepo, J. M., Huck, N., Kessler, S., Gagliardini, V., Gheyselinck, J., Yang, W. C., and Grossniklaus, U. (2007) The FERONIA receptor-like kinase mediates male-female interactions during pollen tube reception. *Science* **317**, 656–660